Kamakhya Prasad Ghatak
Sitangshu Bhattacharya
Debashis De

SPRINGER SERIES IN MATERIALS SCIENCE 116

# Einstein Relation in Compound Semiconductors and Their Nanostructures

Springer

Springer Series in

MATERIALS SCIENCE 116

Springer Series in

# MATERIALS SCIENCE

---

The Springer Series in Materials Science covers the complete spectrum of materials physics, including fundamental principles, physical properties, materials theory and design. Recognizing the increasing importance of materials science in future device technologies, the book titles in this series reflect the state-of-the-art in understanding and controlling the structure and properties of all important classes of materials.

99 **Self-Organized Morphology in Nanostructured Materials**
Editors: K. Al-Shamery and J. Parisi

100 **Self Healing Materials**
An Alternative Approach
to 20 Centuries of Materials Science
Editor: S. van der Zwaag

101 **New Organic Nanostructures for Next Generation Devices**
Editors: K. Al-Shamery, H.-G. Rubahn, and H. Sitter

102 **Photonic Crystal Fibers**
Properties and Applications
By F. Poli, A. Cucinotta, and S. Selleri

103 **Polarons in Advanced Materials**
Editor: A.S. Alexandrov

104 **Transparent Conductive Zinc Oxide**
Basics and Applications
in Thin Film Solar Cells
Editors: K. Ellmer, A. Klein, and B. Rech

105 **Dilute III-V Nitride Semiconductors and Material Systems**
Physics and Technology
Editor: A. Erol

106 **Into The Nano Era**
Moore's Law Beyond Planar Silicon CMOS
Editor: H.R. Huff

107 **Organic Semiconductors in Sensor Applications**
Editors: D.A. Bernards, R.M. Ownes, and G.G. Malliaras

108 **Evolution of Thin-Film Morphology**
Modeling and Simulations
By M. Pelliccione and T.-M. Lu

109 **Reactive Sputter Deposition**
Editors: D. Depla and S. Mahieu

110 **The Physics of Organic Superconductors and Conductors**
Editor: A. Lebed

111 **Molecular Catalysts for Energy Conversion**
Editors: T. Okada and M. Kaneko

112 **Atomistic and Continuum Modeling of Nanocrystalline Materials**
Deformation Mechanisms
and Scale Transition
By M. Cherkaoui and L. Capolungo

113 **Crystallography and the World of Symmetry**
By S.K. Chatterjee

114 **Piezoelectricity**
Evolution and Future of a Technology
Editors: W. Heywang, K. Lubitz, and W. Wersing

115 **Lithium Niobate**
Defects, Photorefraction
and Ferroelectric Switching
By T. Volk and M. Wöhlecke

116 **Einstein Relation in Compound Semiconductors and Their Nanostructures**
By K.P. Ghatak, S. Bhattacharya, and D. De

117 **From Bulk to Nano**
The Many Sides of Magnetism
By C.G. Stefanita

---

Volumes 50–98 are listed at the end of the book.

Kamakhya Prasad Ghatak
Sitangshu Bhattacharya
Debashis De

# Einstein Relation in Compound Semiconductors and Their Nanostructures

With 253 Figures

Springer

Professor Dr. Kamakhya Prasad Ghatak
University of Calcutta, Department of Electronic Science
Acharya Prafulla Chandra Rd. 92, 700 009 Kolkata, India
E-mail: kamakhyaghatak@yahoo.co.in

Dr. Sitangshu Bhattacharya
Nanoscale Device Research Laboratory
Center for Electronics Design Technology
Indian Institute of Science, Bangalore-560012, India
E-mail: isbsin@yahoo.co.in

Dr. Debashis De
West Bengal University of Technology, Department of Computer Sciences and Engineering
700 064 Kolkata, India
E-mail: debashis.de@wbut.ac.in

*Series Editors:*

Professor Robert Hull
University of Virginia
Dept. of Materials Science and Engineering
Thornton Hall
Charlottesville, VA 22903-2442, USA

Professor R. M. Osgood, Jr.
Microelectronics Science Laboratory
Department of Electrical Engineering
Columbia University
Seeley W. Mudd Building
New York, NY 10027, USA

Professor Jürgen Parisi
Universität Oldenburg, Fachbereich Physik
Abt. Energie- und Halbleiterforschung
Carl-von-Ossietzky-Strasse 9–11
26129 Oldenburg, Germany

Professor Hans Warlimont
Institut für Festkörper-
und Werkstofforschung,
Helmholtzstrasse 20
01069 Dresden, Germany

Springer Series in Materials Science ISSN 0933-033X

ISBN 978-3-540-79556-8 e-ISBN 978-3-540-79557-5

Library of Congress Control Number: 2008931052

© Springer-Verlag Berlin Heidelberg 2009

This work is subject to copyright. All rights are reserved, whether the whole or part of the material is concerned, specifically the rights of translation, reprinting, reuse of illustrations, recitation, broadcasting, reproduction on microfilm or in any other way, and storage in data banks. Duplication of this publication or parts thereof is permitted only under the provisions of the German Copyright Law of September 9, 1965, in its current version, and permission for use must always be obtained from Springer-Verlag. Violations are liable to prosecution under the German Copyright Law.

The use of general descriptive names, registered names, trademarks, etc. in this publication does not imply, even in the absence of a specific statement, that such names are exempt from the relevant protective laws and regulations and therefore free for general use.

Typesetting: Data prepared by SPi using a Springer TeX macro package
Cover concept: eStudio Calamar Steinen
Cover production: WMX Design GmbH, Heidelberg

SPIN: 12116942 57/3180/SPi
Printed on acid-free paper

9 8 7 6 5 4 3 2 1

springer.com

# Preface

In recent years, with the advent of fine line lithographical methods, molecular beam epitaxy, organometallic vapour phase epitaxy and other experimental techniques, low dimensional structures having quantum confinement in one, two and three dimensions (such as inversion layers, ultrathin films, nipi's, quantum well superlattices, quantum wires, quantum wire superlattices, and quantum dots together with quantum confined structures aided by various other fields) have attracted much attention, not only for their potential in uncovering new phenomena in nanoscience, but also for their interesting applications in the realm of quantum effect devices. In ultrathin films, due to the reduction of symmetry in the wave–vector space, the motion of the carriers in the direction normal to the film becomes quantized leading to the quantum size effect. Such systems find extensive applications in quantum well lasers, field effect transistors, high speed digital networks and also in other low dimensional systems. In quantum wires, the carriers are quantized in two transverse directions and only one-dimensional motion of the carriers is allowed. The transport properties of charge carriers in quantum wires, which may be studied by utilizing the similarities with optical and microwave waveguides, are currently being investigated. Knowledge regarding these quantized structures may be gained from original research contributions in scientific journals, proceedings of international conferences and various review articles. It may be noted that the available books on semiconductor science and technology cannot cover even an entire chapter, excluding a few pages on the Einstein relation for the diffusivity to mobility ratio of the carriers in semiconductors (DMR). The DMR is more accurate than any one of the individual relations for the diffusivity ($D$) or the mobility ($\mu$) of the charge carriers, which are two widely used quantities of carrier transport in semiconductors and their nanostructures.

It is worth remarking that the performance of the electron devices at the device terminals and the speed of operation of modern switching transistors are significantly influenced by the degree of carrier degeneracy present in these devices. The simplest way of analyzing such devices, taking into account the degeneracy of the bands, is to use the appropriate Einstein relation to express the performances at the device terminals and the switching speed in terms of carrier concentration (S.N. Mohammad, *J. Phys.* ***C***, **13**, 2685 (1980)). It is well known from the fundamental works of Landsberg (P.T. Landsberg, *Proc. R. Soc.* ***A***, **213**, 226, (1952); *Eur. J. Phys*, **2**, 213, (1981)) that the Einstein relation for degenerate materials is essentially determined by their energy band structures. It has, therefore, different values in different materials having various band structures and varies with electron concentration, the magnitude of the reciprocal quantizing magnetic field, the quantizing electric field as in inversion layers, ultrathin films, quantum wires and with the superlattice period as in quantum confined semiconductor superlattices having various carrier energy spectra.

This book is partially based on our on-going researches on the Einstein relation from 1980 and an attempt has been made to present a cross section of the Einstein relation for a wide range of materials with varying carrier energy spectra, under various physical conditions.

In Chap. 1, after a brief introduction, the basic formulation of the Einstein relation for multiband semiconductors and suggestion of an experimental method for determining the Einstein relation in degenerate materials having arbitrary dispersion laws are presented. From this suggestion, one can also experimentally determine another two seemingly different but important quantities of quantum effect devices namely, the Debye screening length and the carrier contribution to the elastic constants. In Chap. 2, the Einstein relation in bulk specimens of tetragonal materials (taking n-$Cd_3As_2$ and n-$CdGeAs_2$ as examples) is formulated on the basis of a generalized electron dispersion law introducing the anisotropies of the effective electron masses and the spin orbit splitting constants respectively together with the inclusion of the crystal field splitting within the framework of the $\boldsymbol{k.p}$ formalism. The theoretical formulation is in good agreement with the suggested experimental method of determining the Einstein relation in degenerate materials having arbitrary dispersion laws. The results of III–V (e.g. InAs, InSb, GaAs, etc.), ternary (e.g. $Hg_{1-x}Cd_xTe$), quaternary (e.g. $In_{1-x}Ga_xAs_{1-y}P_y$ lattice matched to InP) compounds form a special case of our generalized analysis under certain limiting conditions. The Einstein relation in II–VI, IV–VI, stressed Kane type semiconductors together with bismuth are also investigated by using the appropriate energy band structures for these materials. The importance of these materials in the emergent fields of opto- and nanoelectronics is also described in Chap. 2.

The effects of quantizing magnetic fields on the band structures of compound semiconductors are more striking than those of the parabolic one and are easily observed in experiments. A number of interesting physical features originate from the significant changes in the basic energy wave vector relation of the carriers caused by the magnetic field. Valuable information could also be obtained from experiments under magnetic quantization regarding the important physical properties such as Fermi energy and effective masses of the carriers, which affect almost all the transport properties of the electron devices. Besides, the influence of cross-field configuration is of fundamental importance to an understanding of the various physical properties of various materials having different carrier dispersion relations. In Chap. 3, we study the Einstein relation in compound semiconductors under magnetic quantization. Chapter 4 covers the influence of crossed electric and quantizing magnetic fields on the Einstein relation in compound semiconductors. Chapter 5 covers the study of the Einstein relation in ultrathin films of the materials mentioned.

Since Iijima's discovery (S. Iijima, *Nature* **354**, 56 (1991)), carbon nanotubes (CNTs) have been recognized as fascinating materials with nanometer dimensions, uncovering new phenomena in different areas of nanoscience and technology. The remarkable physical properties of these quantum materials make them ideal candidates to reveal new phenomena in nanoelectronics. Chapter 6 contains the study of the Einstein relation in quantum wires of compound semiconductors, together with carbon nanotubes.

In recent years, there has been considerable interest in the study of the inversion layers which are formed at the surfaces of semiconductors in metal–oxide–semiconductor field-effect transistors (MOSFET) under the influence of a sufficiently strong electric field applied perpendicular to the surface by means of a large gate bias. In such layers, the carriers form a two dimensional gas and are free to move parallel to the surface while their motion is quantized in the perpendicular to it leading to the formation of electric subbands. In Chap. 7, the Einstein relation in inversion layers on compound semiconductors has been investigated.

The semiconductor superlattices find wide applications in many important device structures such as avalanche photodiode, photodetectors, electro-optic modulators, etc. Chapter 8 covers the study of the Einstein relation in nipi structures. In Chap. 9, the Einstein relation has been investigated under magnetic quantization in III-V, II-VI, IV-VI, HgTe/CdTe superlattices with graded interfaces. In the same chapter, the Einstein relation under magnetic quantization for effective mass superlattices has also been investigated. It also covers the study of quantum wire superlattices of the materials mentioned. Chapter 10 presents an initiation regarding the influence of light on the Einstein relation in optoelectronic materials and their quantized structures which is itself in the stage of infancy.

In the whole field of semiconductor science and technology, the heavily doped materials occupy a singular position. Very little is known regarding the dispersion relations of the carriers of heavily doped compound semiconductors and their nanostructures. Chapter 11 attempts to touch this enormous field of active research with respect to Einstein relation for heavily doped materials in a nutshell, which is itself a sea. The book ends with Chap. 12, which contains the conclusion and the scope for future research.

As there is no existing book devoted totally to the Einstein relation for compound semiconductors and their nanostructures to the best of our knowledge, we hope that the present book will be a useful reference source for the present and the next generation of readers and researchers of solid state electronics in general. In spite of our joint efforts, the production of error free first edition of any book from every point of view enjoys the domain of impossibility theorem. Various expressions and a few chapters of this book have been appearing for the first time in printed form. The positive suggestions of the readers for the development of the book will be highly appreciated.

In this book, from Chap. 2 to the end, we have presented 116 open and 60 allied research problems in this beautiful topic, as we believe that a proper identification of an open research problem is one of the biggest problems in research. The problems presented here are an integral part of this book and will be useful for readers to initiate their own contributions to the Einstein relation. This aspect is also important for PhD aspirants and researchers. We strongly contemplate that the readers with a mathematical bent of mind would invariably yearn for investigating all the systems from Chapters 2 to 12 and the related research problems by removing all the mathematical approximations and establishing the appropriate respective uniqueness conditions. Each chapter except the last one ends with a table containing the main results.

It is well known that the studies in carrier transport of modern semiconductor devices are based on the Boltzmann transport equation which can, in turn, be solved if and only if the dispersion relations of the carriers of the different materials are known. In this book, we have investigated various dispersion relations of different quantized structures and the corresponding electron statistics to study the Einstein relation. Thus, in this book, the alert readers will find information regarding quantum-confined low-dimensional materials having different band structures. Although the name of the book is extremely specific, from the content one can infer that it will be useful in graduate courses on semiconductor physics and devices in many Universities. Besides, as a collateral study, we have presented the detailed analysis of the effective electron mass for the said systems, the importance of which is already well known, since the inception of semiconductor science. Last but not the least, we do hope that our humble effort will kindle the desire of anyone engaged in materials research and device development, either in academics or in industries, to delve deeper into this fascinating topic.

## Acknowledgments

### Acknowledgment by Kamakhya Prasad Ghatak

I am grateful to A.N. Chakravarti, my Ph.D thesis advisor, for introducing an engineering graduate to the classics of Landau Liftsitz 30 years ago, and with whom I spent countless hours delving into the sea of semiconductor physics. I am also indebted to D. Raychaudhuri for transforming a network theorist into a quantum mechanic. I realize that three renowned books on semiconductor science, in general, and more than 200 research papers of

B.R. Nag, still fire my imagination. I would like to thank P.T. Landsberg, D. Bimberg, W.L. Freeman, B. Podor, H.L. Hartnagel, V.S. Letokhov, H.L. Hwang, F.D. Boer, P.K. Bose, P.K. Basu, A. Saha, S. Roy, R. Maity, R. Bhowmik, S.K. Dasgupta, M. Mitra, D. Chattopadhyay, S.N. Biswas and S.K. Biswas for several important interactions.

I am particularly indebted to K. Mukherjee, A.K. Roy, S.S. Baral, S.K. Roy, R.K. Poddar, N. Guhochoudhury, S.K. Sen, S. Pahari and D.K. Basu, who acted as mentors in the difficult moments of my academic career. I thank my department colleagues and the members of my research team for their help. P.K. Sarkar of the semiconductor device laboratory has always helped me. I am grateful to S. Sanyal for her help and academic advice. I also acknowledge the present Head of the Department, S.N. Sarkar, for creating an environment for the advancement of learning, which is the logo of the University of Calcutta, and helping me to win an award in research and development from the All India Council for Technical Education, India, under which the writing of many chapters of this book became a reality. Besides, this book has been completed under the grant (8023/BOR/RID/RPS-95/2007-08) as sanctioned by the said Council in their research promotion scheme 2008 of the Council.

## Acknowledgment by Sitangshu Bhattacharya

I am indebted to H.S. Jamadagni and S. Mahapatra at the Centre for Electronics Design and Technology (CEDT), Indian Institute of Science, Bangalore, for their constructive guidance in spite of a tremendous research load and to my colleagues at CEDT, for their constant academic help. I am also grateful to my sister, Ms. S. Bhattacharya and my friend Ms. A. Chakraborty for their constant inspiration and encouragement for performing research work even in my tough times, which, in turn, forms the foundation of this twelve-storied book project. I am grateful to my teacher K.P. Ghatak, with whom I work constantly to understand the mysteries of quantum effect devices.

## Acknowledgment by Debashis De

I am grateful to K.P. Ghatak, B.R. Nag, A.K. Sen, P.K. Roy, A.R. Thakur, S. Sengupta, A.K. Roy, D. Bhattacharya, J.D. Sharma, P. Chakraborty, D. Lockwood, N. Kolbun and A.N. Greene. I am highly indebted to my brother S. De for his constant inspiration and support. I must not allow a special thank you to my better half Mrs. S. De, since in accordance with Sanatan Hindu Dharma, the fusion of marriage has transformed us to form a single entity, where the individuality is being lost. I am grateful to the All India Council of Technical Education, for granting me the said project jointly in their research promotion scheme 2008 under which this book has been completed.

## Joint Acknowledgments

The accuracy of the presentation owes a lot to the cheerful professionalism of Dr. C. Ascheron, Senior Editor, Physics Springer Verlag, Ms. A. Duhm, Associate Editor Physics, Springer and Mrs. E. Suer, assistant to Dr. Ascheron. Any shortcomings that remain are our own responsibility.

Kolkata, India
June 2008

*K.P. GHATAK*
*S. BHATTACHARYA*
*D. DE*

# Contents

# List of Symbols

| | |
|---|---|
| $\alpha$ | Band nonparabolicity parameter |
| $a$ | The lattice constant |
| $a_0, b_0$ | The widths of the barrier and the well for superlattice structures |
| $A_0$ | The amplitude of the light wave |
| $\overrightarrow{A}$ | The vector potential |
| $A\left(E, n_z\right)$ | The area of the constant energy 2D wave vector space for ultrathin films |
| $B$ | Quantizing magnetic field |
| $B_2$ | The momentum matrix element |
| $b$ | Bandwidth |
| $c$ | Velocity of light |
| $C_1$ | Conduction band deformation potential |
| $C_2$ | A constant which describes the strain interaction between the conduction and valance bands |
| $\Delta C_{44}$ | Second order elastic constant |
| $\Delta C_{456}$ | Third order elastic constant |
| $\Delta$ | Crystal field splitting constant |
| $\Delta_0$ | Interface width |
| $\Delta\left(\frac{1}{B}\right)$ | Period of SdH oscillation |
| $d_0$ | Superlattice period |
| $D$ | Diffusion constant |
| $\frac{D}{\mu}$ | Einstein relation/diffusivity-mobility ratio in semiconductors |
| $D_0(E)$ | Density-of-states (DOS) function |
| $D_{\mathrm{B}}\left(E\right)$ | Density-of-states function in magnetic quantization |
| $D_{\mathrm{B}}\left(E, \lambda\right)$ | Density-of-states function under the presence of light waves |
| $d_x, d_y, d_z$ | Nanothickness along the $x$, $y$ and $z$-directions |
| $\Delta_{\|\|}$ | Spin–orbit splitting constant parallel to the $C$-axis |
| $\Delta_{\perp}$ | Spin–orbit splitting constant perpendicular to the $C$-axis |
| $\Delta$ | Isotropic spin–orbit splitting constant |

| | |
|---|---|
| $\mathrm{d}^3k$ | Differential volume of the $k$ space |
| $\in$ | Energy as measured from the center of the band gap |
| $\varepsilon$ | Trace of the strain tensor |
| $\varepsilon_0$ | Permittivity of free space |
| $\varepsilon_\infty$ | Semiconductor permittivity in the high frequency limit |
| $\varepsilon_{sc}$ | Semiconductor permittivity |
| $\Delta E_\mathrm{g}$ | Increased band gap |
| $\lvert e\rvert$ | Magnitude of electron charge |
| $E$ | Total energy of the carrier |
| $E_0, \zeta_0$ | Electric field |
| $E_\mathrm{g}$ | Band gap |
| $E_i$ | Energy of the carrier in the $i$th band. |
| $E_\mathrm{ki}$ | Kinetic energy of the carrier in the $i$th band |
| $E_\mathrm{F}$ | Fermi energy |
| $\bar{E}_\mathrm{FB}$ | Fermi energy in the presence of cross-fields configuration |
| $\bar{E}_\mathrm{F0}$ | Fermi energy in the electric quantum limit |
| $\bar{E}_0$ | Energy of the electric sub-band in electric quantum limit |
| $E_\mathrm{FB}$ | Fermi energy in the presence of magnetic quantization |
| $E_n$ | Landau subband energy |
| $E_\mathrm{Fs}$ | Fermi energy in the presence of size quantization |
| $E_\mathrm{Fis}, E_\mathrm{Fiw}$ | Fermi energy under the strong and weak electric field limit |
| $\bar{E}_\mathrm{Fs}, \bar{E}_\mathrm{Fw}$ | Fermi energy in the n-channel inversion layer under the strong and weak electric field quantum limit |
| $\bar{E}_\mathrm{0s}, \bar{E}_\mathrm{0w}$ | Subband energy under the strong and weak electric field quantum limit |
| $\bar{E}_\mathrm{Fn}$ | Fermi energy for nipis |
| $E_\mathrm{FSL}$ | Fermi energy in superlattices |
| $\vec{\varepsilon}_\mathrm{s}$ | Polarization vector |
| $E_\mathrm{FQWSL}$ | Fermi energy in quantum wire superlattices with graded interfaces |
| $E_{\mathrm{F}_\mathrm{L}}$ | Fermi energy in the presence of light waves |
| $E_{\mathrm{F}_\mathrm{BL}}$ | Fermi energy under quantizing magnetic field in the presence of light waves |
| $E_\mathrm{F2DL}$ | 2D Fermi energy in the presence of light waves |
| $E_\mathrm{F1DL}$ | 1D Fermi energy in the presence of light waves |
| $E_{\mathrm{g}_0}$ | Un-perturbed band-gap |
| Erfc | Complementary error function |
| Erf | Error function |
| $E_{\mathrm{F}_\mathrm{h}}$ | Fermi energy of heavily doped materials |
| $\bar{E}_\mathrm{hd}$ | Electron energy within the band gap |
| $F_\mathrm{s}$ | Surface electric field |
| $F(V)$ | Gaussian distribution of the impurity potential |
| $F_j(\eta)$ | One parameter Fermi–Dirac integral of order $j$ |
| $f_0$ | Equilibrium Fermi–Dirac distribution function of the total carriers |

| | |
|---|---|
| $f_{0i}$ | Equilibrium Fermi–Dirac distribution function of the carriers in the $i$th band |
| $g_{\mathrm{v}}$ | Valley degeneracy |
| $G$ | Thermoelectric power under classically large magnetic field |
| $G_0$ | Deformation potential constant |
| $g^*$ | Magnitude of the band edge g-factor |
| $h$ | Planck's constant |
| $\hat{H}$ | Hamiltonian |
| $\hat{H}'$ | Perturbed Hamiltonian |
| $H\left(E - E_n\right)$ | Heaviside step function |
| $\widehat{i},\ \widehat{j}$ and $\widehat{k}$ | Orthogonal triads |
| $i$ | Imaginary unit |
| $I$ | Light intensity |
| $j_{\mathrm{ci}}$ | Conduction current contributed by the carriers of the $i$th band |
| $k$ | Magnitude of the wave vector of the carrier |
| $k_{\mathrm{B}}$ | Boltzmann's constant |
| $\lambda$ | Wavelength of the light |
| $\bar{\lambda}_0$ | Splitting of the two spin-states by the spin–orbit coupling and the crystalline field |
| $\bar{l},\ \bar{m},\ \bar{n}$ | Matrix elements of the strain perturbation operator |
| $L_x,\ L_z$ | Sample length along $x$ and $z$ directions |
| $L_0$ | Superlattices period length |
| $L_{\mathrm{D}}$ | Debye screening length |
| $m_1$ | Effective carrier masses at the band-edge along $x$ direction |
| $m_2$ | Effective carrier masses at the band-edge along $y$ direction |
| $m_3$ | The effective carrier masses at the band-edge along $z$ direction |
| $m_2'$ | Effective-mass tensor component at the top of the valence band (for electrons) or at the bottom of the conduction band (for holes) |
| $m_i^*$ | Effective mass of the $i$th charge carrier in the $i$th band |
| $m_{\|\|}^*$ | Longitudinal effective electron masses at the edge of the conduction band |
| $m_{\perp}^*$ | Transverse effective electron masses at the edge of the conduction band |
| $m^*$ | Isotropic effective electron masses at the edge of the conduction band |
| $m_{\perp,1}^*,\ m_{\|,1}^*$ | Transverse and longitudinal effective electron masses at the edge of the conduction band for the first material in superlattice |
| $m_{\mathrm{r}}$ | Reduced mass |
| $m_0, m$ | Free electron mass |
| $m_{\mathrm{v}}$ | Effective mass of the heavy hole at the top of the valance band in the absence of any field |
| $m,\ n$ | Carbon nanotubes chiral indices |
| $n$ | Landau quantum number |
| $n_x,\ n_y,\ n_z$ | Size quantum numbers along the $x$, $y$ and $z$-directions |

| | |
|---|---|
| $n_{1\mathrm{D}},\ n_{2\mathrm{D}}$ | 1D and 2D carrier concentration |
| $n_{2\mathrm{Ds}},\ n_{2\mathrm{Dw}}$ | 2D surface electron concentration under strong and weak electric field |
| $\bar{n}_{2\mathrm{Ds}},\ \bar{n}_{2\mathrm{Dw}}$ | Surface electron concentration under the strong and weak electric field quantum limit |
| $n_i$ | Miniband index for nipi structures |
| $N_{\mathrm{nipi}}\,(E)$ | Density-of-states function for nipi structures |
| $N_{2\mathrm{DT}}\,(E)$ | 2D Density-of-states function |
| $N_{2\mathrm{D}}\,(E, \lambda)$ | 2D density-of-states function in the presence of light waves |
| $N_{1\mathrm{D}}\,(E, \lambda)$ | 1D density-of-states function in the presence of light waves |
| $n_0$ | Total electron concentration |
| $\bar{n}_0$ | Electron concentration in the electric quantum limit |
| $n_i$ | Carrier concentration in the $i$th band |
| $P$ | Isotropic momentum matrix element |
| $P_n$ | Available noise power |
| $P_{\vert\vert}$ | Momentum matrix elements parallel to the direction of crystal axis |
| $P_{\perp}$ | Momentum matrix elements perpendicular to the direction of crystal axis |
| $\vec{\boldsymbol{r}}$ | Position vector |
| $S_i$ | Zeros of the airy function |
| $\vec{\boldsymbol{s}}_{\mathbf{0}}$ | Momentum vector of the incident photon |
| $t$ | Time scale |
| $t_{\mathrm{c}}$ | Tight binding parameter |
| $T$ | Absolute temperature |
| $\tau_i\,(E)$ | Relaxation time of the carriers in the $i$th band |
| $u_1(\vec{k}, \vec{r}), u_2(\vec{k}, \vec{r})$ | Doubly degenerate wave functions |
| $V\,(E)$ | Volume of $k$ space |
| $V_0$ | Potential barrier encountered by the electron |
| $V(\vec{r})$ | Crystal potential |
| $x,\ y$ | Alloy compositions |
| $z_{\mathrm{t}}$ | Classical turning point |
| $\mu_i$ | Mobility of the carriers in the $i$th band |
| $\mu$ | Average mobility of the carriers |
| $\zeta(2r)$ | Zeta function of order $2r$ |
| $\Gamma\,(j+1)$ | Complete Gamma function |
| $\eta$ | Normalized Fermi energy |
| $\eta_{\mathrm{g}}$ | Impurity scattering potential |
| $\omega_0$ | Cyclotron resonance frequency |
| $\theta$ | Angle |
| $\mu_0$ | Bohr magnetron, |
| $\omega$ | Angular frequency of light wave |
| $\uparrow', \downarrow'$ | Spin up and down function |

# 1

# Basics of the Einstein Relation

## 1.1 Introduction

It is well known that the Einstein relation for the diffusivity-mobility ratio (DMR) of the carriers in semiconductors occupies a central position in the whole field of semiconductor science and technology [1] since the diffusion constant (a quantity very useful for device analysis where exact experimental determination is rather difficult) can be obtained from this ratio by knowing the experimental values of the mobility. The classical value of the DMR is equal to $(k_{\mathrm{B}}T \,/\, |e|)$, ($k_{\mathrm{B}}$, $T$, and $|e|$ are Boltzmann's constant, temperature and the magnitude of the carrier charge, respectively). This relation in this form was first introduced to study the diffusion of gas particles and is known as the Einstein relation [2,3]. Therefore, it appears that the DMR increases linearly with increasing $T$ and is independent of electron concentration. This relation holds for both types of charge carriers only under non-degenerate carrier concentration although its validity has been suggested erroneously for degenerate materials [4]. Landsberg first pointed out that the DMR for semiconductors having degenerate electron concentration are essentially determined by their energy band structures [5, 6]. This relation is useful for semiconductor homostructures [7, 8], semiconductor–semiconductor heterostructures [9, 10], metals–semiconductor heterostructures [11–19] and insulator–semiconductor heterostructures [20–23]. The nature of the variations of the DMR under different physical conditions has been studied in the literature [1–3, 5, 6, 24–50] and some of the significant features, which have emerged from these studies, are:

(a) The ratio increases monotonically with increasing electron concentration in bulk materials and the nature of these variations are significantly influenced by the energy band structures of different materials;
(b) The ratio increases with the increasing quantizing electric field as in inversion layers;

(c) The ratio oscillates with the inverse quantizing magnetic field under magnetic quantization due to the Shubnikov de Hass effect;
(d) The ratio shows composite oscillations with the various controlled quantities of semiconductor superlattices.
(e) In ultrathin films, quantum wires and field assisted systems, the value of the DMR changes appreciably with the external variables depending on the nature of quantum confinements of different materials.

Before the in depth study of the aforementioned cases, the basic formulation of the DMR for multi-band non-parabolic degenerate materials has been presented in Sect. 1.2. Besides, the suggested experimental method of determining the DMR for materials having arbitrary dispersion laws has also been included in Sect. 1.3.

## 1.2 Generalized Formulation of the Einstein Relation for Multi-Band Semiconductors

The carrier energy spectrum in the $i$th band in multi-band semiconducting materials can be expressed as [31]

$$E = \left( \frac{\hbar^2 k^2}{2m_i^*(E)} \right) + E_i = E_{\mathrm{ki}} + E_i, \tag{1.1}$$

where $E$ is the total energy of the carrier as measured from the edge of the band in the vertically upward direction, $\hbar = h / 2\pi, h$ is Planck constant, $k$ is the magnitude of the wave vector of the carrier, $m_i^*(E)$ is the effective mass of the charge carrier, $E_i$ is the energy of the carrier in the $i$th band in the $z$-direction and $E_{\mathrm{ki}}$ is the kinetic energy of the carrier in the $i$th band.

The carrier concentration $n_i$ in the $i$th band can be written as

$$n_i(E_{\mathrm{Fi}}) = (4\pi^3)^{-1} \int f_{0i}\, \mathrm{d}^3 k, \tag{1.2}$$

where $E_{\mathrm{Fi}} = E_{\mathrm{F}} - E_i, E_{\mathrm{F}}$ is the Fermi energy, $f_{0i}$ the Fermi–Dirac equilibrium distribution function of the carriers in the $i$th band can, in turn, be expressed as

$$f_{0i} = \left[1 + \exp\left[(k_{\mathrm{B}}T)^{-1}(E_{\mathrm{ki}} + E_i - E_{\mathrm{F}})\right]\right]^{-1}, \tag{1.3}$$

and $\mathrm{d}^3 k$ is the differential volume of $k$ space.

The solution of the Boltzmann transport equation under relaxation time approximation leads to the expression of the conduction current $j_{\mathrm{ci}}$ contributed by the carriers in the $i$th band in the presence of an electric field $\zeta_0$ in the $z$-direction as given by [31]

$$j_{\mathrm{ci}} = -\left(4\pi^3\right)^{-1}\left(\zeta_0 e^2 / \hbar^2\right) \int \left(\nabla_{kz} E\right)^2 \tau_i(E)\left(\partial f_{0i} / \partial E_{\mathrm{ki}}\right) \mathrm{d}^3 k = |e|\left(n_i \mu_i \zeta_0\right), \tag{1.4}$$

where $\mu_i$ is the mobility and $\tau_{\mathrm{i}}(E)$ is the relaxation time. For scattering mechanisms, for which the relaxation time approximation is invalid, (1.4) remains invariant where $\tau_{\mathrm{i}}(E)$ is being replaced by $\phi_i(E)$. The perturbation in the distribution function can be written as

$$f_i \equiv f_{0i} - \left[(\nabla_{k_z} E)\left(\frac{\partial f_{0i}}{\partial E_{\mathrm{ki}}}\right)\phi_i(E)\right]\left(\frac{e\zeta_0}{\hbar}\right),$$

The current density due to conduction mechanism can be expressed as

$$J_c = |e| \sum_i n_i \mu_i \zeta_0 = |e|\, \mu n_0 \zeta_0,$$

where $\mu$ is the average mobility of the carriers and $n_0$ is the total electron concentration defined by $n_0 = \sum\limits_i n_i$.

It may be noted that the diffusion current density will also exist when the carrier concentration varies with the position and consequently the concentration gradient is being created. Let us assume that it varies along the $z$-direction, under these conditions, both $E_{\mathrm{F}}$ and $E_i$ will in general be functions of $z$. The application of the same process leads to the expression of the diffusion current density contributed by the carriers in the $i$th band as

$$j_{\mathrm{Di}} = -\left(4\pi^3\right)^{-1}\left(\frac{e}{\hbar^2}\right)\int (\nabla_{k_z} E)^2 \tau_i(E)\left(\frac{\partial f_{0i}}{\partial z}\right) \mathrm{d}^3 k, \tag{1.5}$$

We note that

$$\frac{\partial f_{0i}}{\partial z} = \frac{\partial f_{0i}}{\partial E_{\mathrm{Fi}}}\frac{\partial E_{\mathrm{Fi}}}{\partial z} = -\frac{\partial f_{0i}}{\partial E_{\mathrm{ki}}}\frac{\partial E_{\mathrm{Fi}}}{\partial z},$$

and

$$\frac{\partial n}{\partial z} = \frac{\partial}{\partial z}\sum_i n_i\left(E_{\mathrm{Fi}}\right) = \frac{\partial E_{\mathrm{Fi}}}{\partial z}\beta_i, \tag{1.6}$$

where

$$\beta_i = \sum_j \frac{\partial n_j\left(E_{\mathrm{Fi}}\right)}{\partial E_{\mathrm{Fj}}}\frac{\partial E_{\mathrm{Fj}}}{\partial E_{\mathrm{Fi}}} \tag{1.7}$$

in which $j$ stands for the $j$th band.

Using (1.5), (1.6) and (1.7), one can write

$$J_{\mathrm{Di}} = \frac{1}{4\pi^3}\frac{e}{\hbar^2}\frac{\partial n_0}{\partial z}\int (\nabla_{k_z} E)^2 \tau_i(E)\frac{\partial f_{0i}}{\partial E_{ki}}\beta_i^{-1}\,\mathrm{d}^3 k = -\frac{e}{|e|}\frac{\partial n_0}{\partial z} n_i \mu_i \beta_i^{-1}. \tag{1.8}$$

Hence the total diffusion current is given by

$$j_D = \sum_i j_{\mathrm{Di}} = -\left(\frac{e}{|e|}\right)\left(\frac{\partial n_0}{\partial z}\right)\sum_i n_i \mu_i (\beta_i)^{-1} = -De\left(\frac{\partial n_0}{\partial z}\right), \tag{1.9a}$$

where $D$ is the diffusion constant.

Thus, we get [31]

$$D = \frac{1}{|e|}\left[\sum_i n_i \mu_i \left(\beta_i\right)^{-1}\right] \tag{1.9b}$$

and

$$\frac{D}{\mu} = \left[\frac{1}{|e|}\right] n_0 \frac{\sum\limits_i n_i \mu_i \beta_i^{-1}}{\sum\limits_i n_i \mu_i} \tag{1.10}$$

When $E_i$s are $z$ invariant, (1.10) assumes the well known form as [31]

$$\frac{D}{\mu} = \left(\frac{n_0}{|e|}\right) / \left(\frac{\mathrm{d}n_0}{\mathrm{d}E_F}\right). \tag{1.11}$$

The electric quantum limit as in inversion layers and nipi structures refers to the lowest electric sub-band and for this particular case $i = j = 0$. Therefore, (1.10) can be written as

$$\frac{D}{\mu} = \left(\frac{\bar{n}_0}{|e|}\right) / \left(\frac{\mathrm{d}\bar{n}_0}{\mathrm{d}\left(\bar{E}_{F0} - \bar{E}_0\right)}\right), \tag{1.12}$$

where $\bar{n}_0$, $\bar{E}_{F0}$ and $\bar{E}_0$ are the electron concentration, the energy of the electric sub-band and the Fermi energy in the electric quantum limit.

It should be noted that (1.11) is valid for different kinds of multi-band materials and low dimensional systems if the contribution of the charge density to the internal potential is small except for inversion layers and nipi structures. For these cases (1.10) should be used for the evaluation of DMR. For inversion layers and nipis under the electric quantum limit and for heavily doped semiconductors, (1.12) may be used.

## 1.3 Suggestions for the Experimental Determination of the Einstein Relation in Semiconductors Having Arbitrary Dispersion Laws

(a) It is well-known that the thermoelectric power of the carriers in semiconductors in the presence of a classically large magnetic field is independent of scattering mechanisms and is determined only by their energy band spectra [51]. The magnitude of the thermoelectric power $G$ can be written as [51]

$$G = \frac{1}{|e|\, T n_0} \int\limits_{-\infty}^{\infty} \left(E - E_{\mathrm{F}}\right) R\left(E\right) \left[-\frac{\partial f_0}{\partial E}\right] \mathrm{d}E, \tag{1.13}$$

where $R\left(E\right)$ is the total number of states. Equation (1.13) can be written under the condition of carrier degeneracy [52, 53] as

$$G = \left(\frac{\pi^2 {k_B}^2 T}{3\left|e\right| n_0}\right)\left(\frac{\partial n_0}{\partial E_F}\right). \tag{1.14}$$

The use of (1.11) and (1.14) leads to the result [52]

$$\frac{D}{\mu} = \left(\frac{\pi^2 {k_B}^2 T}{3\left|e\right|^2 G}\right). \tag{1.15}$$

Thus, the DMR for degenerate materials can be determined by knowing the experimental values of $G$.

The suggestion for the experimental determination of the DMR for degenerate semiconductors having arbitrary dispersion laws as given by (1.15) does not contain any energy band constants. For a fixed temperature, the DMR varies inversely as $G$. Only the experimental values of $G$ for any material as a function of electron concentration will generate the experimental values of the DMR for that range of $n_0$ for that system. Since $G$ decreases with increasing $n_0$, from (1.15) one can infer that the DMR will increase with increase in $n_0$. This statement is the compatibility test so far as the suggestion for the experimental determination of DMR for degenerate materials is concerned.

(b) For inversion layers and the nipi structures, under the condition of electric quantum limit, (1.13) assumes the form

$$G = \left(\frac{\pi^2 {k_B}^2 T}{3\left|e\right| \bar{n}_0}\right)\left[\frac{\mathrm{d}\bar{n}_0}{\mathrm{d}\left(\bar{E}_{F0} - \bar{E}_0\right)}\right]. \tag{1.16}$$

Using (1.16) and (1.12) one can again obtain the same (1.15). For quantum wires and heterostructures with small charge densities, the relation between $D/\mu$ and $G$ is thus given by (1.15). Equation (1.15) is also valid under magnetic quantization and also for cross-field configuration. Thus, (1.15) is independent of the dimensions of quantum confinement. We should note that the present analysis is not valid for totally $k$-space quantized systems such as quantum dots, magneto-inversion and accumulation layers, magneto size quantization, magneto nipis, quantum dot Superlattices and quantum well Superlattices under magnetic quantization. Under the said conditions, the electron motion is possible in the broadened levels. The experimental results of $G$ for degenerate materials will provide an experimental check on the DMR and also a technique for probing the band structure of degenerate compounds having arbitrary dispersion laws.

(c) In accordance with Nag and Chakravarti [32]

$$\frac{D}{\mu} = P_n \left|e\right| b, \tag{1.17}$$

where $P_n$ is the available noise power in the band width $b$. We wish to remark that (1.17) is valid only for semiconductors having non-degenerate electron concentration, whereas the compound small gap semiconductors are degenerate in general.

(d) In this context, it may be noted that the results of this section find the following two important applications in the realm of quantum effect devices:

(1) It is well known that the Debye screening length (DSL) of the carriers in the semiconductors is a fundamental quantity, characterizing the screening of the Coulomb field of the ionized impurity centers by the free carriers. It affects many special features of the modern semiconductor devices, the carrier mobilities under different mechanisms of scattering, and the carrier plasmas in semiconductors [53–55]. The DSL ($L_{\mathrm{D}}$)can, in general, be written as [54–56]

$$L_{\mathrm{D}} = \left( \frac{|e|^2}{\varepsilon_{\mathrm{sc}}} \frac{\partial n_0}{\partial E_{\mathrm{F}}} \right)^{-1/2}, \tag{1.18}$$

where $\varepsilon_{\mathrm{sc}}$ is the semiconductor permittivity.

Using (1.18) and (1.14), one obtains

$$L_{\mathrm{D}} = \left( 3\,|e|^3\, n_0 G \,/\, \varepsilon_{\mathrm{sc}} \pi^2 k_{\mathrm{B}}^2 T \right)^{-1/2}. \tag{1.19}$$

Therefore, we can experimentally determine $L_D$ by knowing the experimental curve of $G$ vs. $n_0$ at a fixed temperature.

(2) The knowledge of the carrier contribution to the elastic constants are useful in studying the mechanical properties of the materials and has been investigated in the literature [57–60]. The electronic contribution to the second- and third-order elastic constants can be written as [57–60]

$$\Delta C_{44} = -\frac{G_0^2}{9} \frac{\partial n_0}{\partial E_{\mathrm{F}}}, \tag{1.20}$$

and

$$\Delta C_{456} = \frac{G_0^3}{27} \frac{\partial^2 n_0}{\partial E_{\mathrm{F}}^2}, \tag{1.21}$$

where $G_0$ is the deformation potential constant. Thus, using (1.14), (1.20) and (1.21), we can write

$$\Delta C_{44} = \left[ -n_0 G_0^2\, |e|\, G \,/\, \left( 3\pi^2 k_{\mathrm{B}}^2 T \right) \right], \tag{1.22}$$

and

$$\Delta C_{456} = \left( n_0\, |e|\, G_0^3 G^2 \,/\, (3\pi^4 k_{\mathrm{B}}^3 T) \right) \left( 1 + \frac{n_0}{G} \frac{\partial G}{\partial n_0} \right). \tag{1.23}$$

Thus, again the experimental graph of $G$ vs. $n_0$ allows us to determine the electronic contribution to the elastic constants for materials having arbitrary spectras.

## 1.4 Summary

Section 1.2 of this chapter presents the expression of the Einstein relation together with the special practical cases. The formulation of the Einstein relation requires the relation between the electron concentration and the Fermi energy, which, in turn, is determined by the respective energy band structure. For various materials the electron dispersion relations are different and consequently all the subsequent formulations change radically introducing new information. The dispersion relation for bulk materials gets modified under magnetic quantization, in inversion layers, ultrathin films, quantum wires, and with various types of semiconductor superlattices. The electron energy spectrum also changes in a fundamental way for heavily doped semiconductors and also in the presence of external photo-excitation, respectively. We shall study these aspects in the incoming chapters. The experimental determination of DMR has been investigated in Sect. 1.3 for materials having arbitrary band structures and this suggestion is dimension independent. Besides, the experimental methods for determining the Debye screening length and the

**Table 1.1.** Main results of Chap. 1

(a) The generalized expression for the DMR can be written as

$$\frac{D}{\mu} = \left(\frac{1}{|e|}\right) n_0 \frac{\sum\limits_i n_i \mu_i \beta_i^{-1}}{\sum\limits_i n_i \mu_i}, \tag{1.10}$$

For $E_i$'s independent of $z$, (1.10) gets simplified to the well-known form as

$$\frac{D}{\mu} = \left(\frac{n_0}{|e|}\right) / \left(\frac{\mathrm{d}n_0}{\mathrm{d}E_\mathrm{F}}\right). \tag{1.11}$$

For inversion layers and nipis under electric quantum limit, (1.10) transforms into the form

$$\frac{D}{\mu} = \left(\frac{\bar{n}_0}{|e|}\right) / \left(\frac{\mathrm{d}\bar{n}_0}{\mathrm{d}\left(\bar{E}_{\mathrm{F}0} - \bar{E}_0\right)}\right). \tag{1.12}$$

(b) The DMR, the screening length and the carrier contribution to the elastic constants can be experimentally determined by knowing the experimental curve of the thermoelectric power under large magnetic field vs. the carrier concentration as given by the following, respectively.

$$\frac{D}{\mu} = \left(\frac{\pi^2 k_\mathrm{B}^2 T}{3\,|e|^2\, G}\right), \tag{1.15}$$

$$L_\mathrm{D} = \left(3\,|e|^3\, n_0 G \,/\, \varepsilon_\mathrm{sc} \pi^2 k_\mathrm{B}^2 T\right)^{-1/2}, \tag{1.19}$$

$$\Delta C_{44} = [-n_0 G_0^2\, |e|\, G \,/\, (3\pi^2 k_\mathrm{B}^2 T)], \tag{1.22}$$

$$\Delta C_{456} = \left(n_0\, |e|\, G_0^3 G^2 \,/\, (3\pi^4 k_\mathrm{B}^3 T)\right) \left(1 + \frac{n_0}{G} \frac{\partial G}{\partial n_0}\right), \tag{1.23}$$

carrier contribution to the elastic constants have also been suggested in this context. As a condensed presentation, the main results have been presented in Table 1.1.

## References

1. H. Kroemer, IEEE Trans. Electron Devices **25**, 850 (1978)
2. A. Einstein, Ann. der Physik **17**, 549 (1905); W. Nernst, Z. Phys. Chem. Leipzig **2**, 613 (1888); J.S. Townsend, Trans. R. Soc. **193A**, 129 (1900)
3. C. Wagner, Z. Physik. Chem. **B21**, 24 (1933); C. Herring, M.H. Nichols, Rev. Mod. Phys. **21**, 185 (1949); P.T. Landsberg, *Thermodynamics and Statistical Mechanics.* (Oxford University Press, Oxford, 1978); *In Recombination in Semiconductors.* (Cambridge University Press, UK, 1991)
4. R.W. Lade, Proc. IEEE **52**, 743 (1965)
5. P.T. Landsberg, Proc. R. Soc. **A 213**, 226 (1952); Proc. Phys. Soc. **A 62**, 806 (1949)
6. P.T. Landsberg, Eur. J. Phys **2**, 213 (1981)
7. C.H. Wang, A. Neugroschel, IEEE Electron. Dev. Lett. **ED-11**, 576 (1990)
8. I.-Y. Leu, A. Neugroschel, IEEE Trans. Electron. Dev. **ED-40**, 1872 (1993)
9. F. Stengel, S.N. Mohammad, H. Morkoç, J. Appl. Phys. **80**, 3031 (1996)
10. H.-J. Pan, W.-C. Wang, K.-B. Thai, C.-C. Cheng, K.-H. Yu, K.-W. Lin,C.-Z. Wu, W.-C. Liu, Semiconduct. Sci. Technol. **15**, 1101 (2000)
11. S.N. Mohammad, J. Appl. Phys. **95**, 4856 (2004)
12. V.K. Arora, Appl. Phys. Lett. **80**, 3763 (2002)
13. S.N. Mohammad, J. Appl. Phys. **95**, 7940 (2004)
14. S.N. Mohammad, Philos. Mag. **84**, 2559 (2004)
15. S.N. Mohammad, J. Appl. Phys. **97**, 063703 (2005)
16. K. Suzue, S.N. Mohammad, Z.F. Fan, W. Kim, O. Aktas, A.E. Botchkarev, H. Morkoç, J. Appl. Phys. **80**, 4467 (1996)
17. S.N. Mohammad, Z.F. Fan, W. Kim, O. Aktas, A.E. Botchkarev, A. Salvador, H. Morkoç, Electron. Lett. **32**, 598 (1996)
18. Z. Fan, S.N. Mohammad, W. Kim, O. Aktas, A.E. Botchkarev, K. Suzue, H. Morkoç, J. Electron. Mater. **25**, 1703 (1996)
19. C. Lu, H. Chen, X. Lv, X. Xia, S.N. Mohammad, J. Appl. Phys. **91**, 9216 (2002)
20. S.G. Dmitriev, Yu.V. Markin, Semiconductors **34**, 931 (2000)
21. M. Tao, D. Park, S.N. Mohammad, D. Li, A.E. Botchkerav, H. Morkoç, Philos. Mag. B **73**, 723 (1996)
22. D.G. Park, M. Tao, D. Li, A.E. Botchkarev, Z. Fan, S.N. Mohammad, H. Morkoç, J. Vac. Sci. Technol. B **14**, 2674 (1996)
23. Z. Chen, D.G. Park, S.N. Mohammad, H. Morkoç, Appl. Phys. Lett. **69**, 230 (1996)
24. P.T. Landsberg, J. Appl. Phys. **56**, 1696 (1984); P.T. Landsberg, A.G. Guy, Phys. Rev. B **28**, 1187 (1983); P.T. Landsberg, Phys. Rev. B **33**, 8321 (1986); S.A. Hope, G. Feat, P.T. Landsberg, J. Appl. Phys. **61**, 4909 (1987); Y. Roichman, N. Tessler, Appl. Phys. Lett. **80**, 1948 (2002); J.M.H. Peters, Eur. J. Phys. **3**, 19 (1982); H. Van Cong, S. Brunet, S. Charar, Phys. Stat. Solidi B **109**, K1 (1982); H. Van Cong, Phys. Stat. Solidi A **56**, 395 (1979); H. Van Cong, Solid State Electron. **24**, 495 (1981)

25. S.N. Mohammad, S.T.H. Abidi, J. Appl. Phys. **61**, 4909 (1987); S.N. Mohammad, S.T.H. Abidi, Solid State Electron. **27**, 1153 (1985); S.N. Mohammad, S.T.H. Abidi, J. Appl. Phys. **56**, 3341 (1984); M.A. Sobhan, S.N. Mohammad, J. Appl. Phys. **58**, 2634 (1985); S.N. Mohammad, A.V. Bemis, IEEE Trans. Electron. Dev. **ED-39**, 282 (1992); S.N. Mohammad, R.L. Carter, Philos. Mag. B **72**, 13 (1995); S.N. Mohammad, Solid State Electron. **46**, 203 (2002); S.N. Mohammad, J. Chen, J.-I. Chyi, H. Morkoç, Appl. Phys. Lett. **56**, 937 (1990)
26. P.T. Landsberg, S.A. Hope, Solid State Electron. **20**, 421 (1977); S.A. Hope, G. Feat, P.T. Landsberg, J. Phys. A. Math. Gen. **14**, 2377 (1981)
27. W. Elsäber, E.O. Göbel, Electron. Lett. **19**, 335 (1983); R. Hilfer, A. Blumen, Phys. Rev. A **37**, 578 (1988); T.G. Castner, Phys. Rev. B **55**, 4003 (1997); E. Barkai, V.N. Fleurov, Phys. Rev. E. **58**, 1296 (1998); Y.Y. Roichman, N. Tessler, Appl. Phys. Lett. **80**, 1948 (2002); T.H. Nguyen, S.K. O'Leary, Appl. Phys. Lett. **83**, 1998 (2003); T.H. Nguyen, S.K. O'Leary, J. Appl. Phys. **98**, 076102 (2005); C.G. Rodrigues, Á.R. Vasconcellos, R. Luzzi, J. Appl. Phys. **99**, 073701 (2006)
28. R.K. Jain, Phys. Stat. Sol. (a) **42**, K221 (1977); B.A. Aronzon, E.Z. Meilikhov, Phys. Stat. Sol. (a)**19**, 313 (1973)
29. A.N. Chakravarti, B.R. Nag, Int. J. Electron. **37**, 281 (1974); P.N. Butcher, A.N. Chakravarti, S. Swaminathan, Phys. Stat. Sol. (a) **25**, K47 (1974)
30. B.R. Nag, A.N. Chakravarti, Solid State Electron. **18**, 109 (1975); B.R. Nag, A.N. Chakravarti, Phys. Stat. Sol. (a) **22**, K153 (1974)
31. B.R. Nag, A.N. Chakravarti, P.K. Basu, Phys. Stat. Sol. (a) **68**, K75 (1981)
32. B.R. Nag, A.N. Chakravarti, Phys. Stat Sol. (a) **67**, K113 (1981)
33. A.N. Chakravarti, D.P. Parui, Phys. Lett. **40A**, 113 (1972); A.N. Chakravarti, D.P. Parui, Phys. Lett. **43A**, 60 (1973); A.N. Chakravarti, D.P. Parui, Phys. Stat. Sol. (a) **14**, K23 (1972); A.N. Chakravarti, D.P. Parui, Phys. Stat. Sol. (a) **14**, K55 (1972); A.N. Chakravarti, D.P. Parui, Canad. J. Phys. **51**, 451 (1973); D. Mukherjee, A.N. Chakravarti, B.R. Nag, Phys. Stat. Sol (a) **26**, K27 (1974); S. Ghosh, A.N. Chakravarti, Phys. Stat. Sol. (b), **147**, 355 (1988)
34. S. Choudhury, D. De, S. Mukherjee, A. Neogi, A. Sinha, M. Pal, S. K. Biswas, S. Pahari, S. Bhattacharya, K.P. Ghatak, J. Comp. Theo. Nanosci. **5**, 375 (2008); S. Mukherjee, S.N. Mitra, P.K. Bose, A.R. Ghatak, A. Neogi, J.P. Banerjee, A. Sinha, M. Pal, S. Bhattacharya, K.P. Ghatak, J. Comp. Theo. Nanosci. **4**, 550 (2007); A. Khan, A. Das, Appl. Phys. A **89**, 695 (2007)
35. J.P. Bouchaud, A. Georges, Phys. Rep. **195**, 127 (1996); V. Blickle, T. Speck, C. Lutz, U. Seifert, C. Bechinger, Phys. Rev. Lett. 98, 210601 (2007); Y. Kang, E. Jean, C.M. Fortmonn, Appl. Phys. Lett. **88**, 112110 (2006); F. Neumann, Y.A. Genenko, H.V. Seggern, J. Appl. Phys. **99**, 013704 (2006); J. van de Lagemaat, Phys. Rev. B. **73**, 235319 (2005); Q. Gu, E.A. Schiff, S. Grneber, F. Wang, R. Schwarz, Phys. Rev. Lett. **76**, 3196 (1996); M.Y. Azbel, Phys. Rev. B. **46**, 15004 (1992)
36. A.H. Marshak, Solid State Electron. **30**, 1089 (1987); A.H. Marshak, C.M.V. Vliet, Proc. IEEE **72**, 148 (1984); C.M.V. Vliet, A. van der Zeil, Solid State Electron. **20**, 931 (1977)
37. A.N. Chakravarti, K.P. Ghatak, A. Dhar, K.K. Ghosh, S. Ghosh, Appl. Phys. **A26**, 169 (1981)
38. B.R. Nag, *Electron Transport in Compound Semiconductors*. (Springer-Verlag, Germany, 1980); O. Madelung, *Semiconductors: Data Handbook*, 3rd edn.

(Springer, Berlin, 2004); M. Krieehbaum, P. Kocevar, H. Pascher, G. Bauer, *IEEE QE* **24**, 1727 (1988)
39. K.P. Ghatak, S.N. Biswas, Nanostruct. Mater. **2**, 91 (1993); K.P. Ghatak, S.N. Biswas, J. Appl. Phys. **70**, 4309 (1991); K.P. Ghatak, B. Mitra, M. Mondal, Ann. der Physik **48**, 283 (1991); B. Mitra, K.P. Ghatak, Physica Scripta **42**, 103 (1990); B. Mitra, K.P. Ghatak, in Phys. Lett. **135A**, 397 (1989); M. Mondal, K.P. Ghatak, Ann. der Physik **46**, 502 (1989); K.P. Ghatak, N. Chattopadhyay, M. Mondal, J. Appl. Phys. **63**, 4536 (1988); J. Low Temp. Phys. **73**, 321 (1988)
40. K.P. Ghatak, A. Ghoshal, S.N. Biswas, Nouvo Cimento **15D**, 39 (1993)
41. K.P. Ghatak, D. Bhattacharyya, Phys. Lett. **A 184**, 366 (1994)
42. K.P. Ghatak, D. Bhattacharyya, Physica Scripta **52**, 343 (1995); M. Mondal, K.P. Ghatak, J. Mag. Mag. Mater. **62**, 115 (1986)
43. K.P. Ghatak, B. Nag, D. Bhattacharyya, J. Low Temp. Phys. **14**, 1 (1995)
44. K.P. Ghatak, M. Mondal, Thin Solid Films **148**, 219 (1987)
45. K.P. Ghatak, A.K. Choudhury, S. Ghosh, A.N. Chakravarti, Appl. Phys. **23**, 241 (1980)
46. K.P. Ghatak, Influence of band structure on some quantum processes in tetragonal semiconductors, D. Eng. Thesis, Jadavpur University, Kolkata, India, 1991
47. K.P. Ghatak, N. Chattopadhyay, M. Mondal, Appl. Phys. A **44**, 305 (1987)
48. S.N. Biswas, K.P. Ghatak, in *Proceedings of the Society of Photo-optical and Instrumentation Engineers (SPIE)*, Quantum Well and Superlattice Physics, USA, 1987, vol. 792, p. 239; K.P. Ghatak, M. Mondal, S. Bhattacharyya, SPIE, USA, 1990, vol. 1284, p. 113; K.P. Ghatak, S. Bhattacharyya, M. Mondal, SPIE, USA, 1990, vol. 1307, p. 588; K.P. Ghatak, B. De, Defect engineering in semiconductor growth, processing and device technology materials research society proceedings (MRS) Spring meeting, 1992, vol. 262, p. 911; K.P. Ghatak, B. De, The Proceedings of Wide Band Gap Semiconductors Symposium, MRS, 1992, p. 377; S. Bhattacharya, K.P. Ghatak, S.N. Biswas, SPIE, 836, Optoelectronic materials, Devices, Packaging Interconnects, 1988, pp. 72–87
49. M. Mondal, K.P. Ghatak, J. Phys. C (Sol. State.) **20**, 1671 (1987); M. Mondal, S.N. Banik, K.P. Ghatak, Canad. J. Phys. **67**, 72 (1989)
50. K.P. Ghatak, M. Mondal, J. Appl. Phys. **70**, 1277 (1992)
51. W. Zawadzki, Adv. Phys. **23**, 435 (1974); B.M. Askerov, N.F. Gashimzade, M.M. Panakhov, Sov. Phys. Solid State **29**, 465 (1987); S.P. Zelenin, A.S. Kondratev, A.I. Kuchma, Sov. Phys. Semicond. **16**, 355 (1982); A.V. Germaneko, G.M. Minkov, Phys. Stat. Sol. (b) **184**, 9 (1994); W. Zawadzki, in *Two-Dimensional Systems, Hetrostructures and Superlattices*, vol. 53, ed. by G. Bower, F. Kuches, H. Haiunich, Springer Ser. Solid-State Sci. (Springer, Berlin, 1984), p. 79; B. Mitra, K.P. Ghatak, Phys. Lett. **141**, 81 (1989); L.J. Singh, S. Choudhury, D. Baruah, S.K. Biswas, S. Pahari, K.P. Ghatak, Physica B **368**, 188 (2005); K.P. Ghatak, B. De, B. Nag, P.K. Chakraborty, Nonlin. Opt. Quant. Opt. **16**, 212 (1996); K.P. Ghatak, M. Mitra, B. Goswami, B. Nag, Nonlin. Opt. **16**, 167 (1996); K.P. Ghatak, B. Nag, Nanostruct. Mater. **2**, 14 (1995); K.P. Ghatak, B. Mitra, Nouvo Cimento **15D**, 97 (1993)
52. S.K. Biswas, A.R. Ghatak, A. Neogi, A. Sharma, S. Bhattacharya, K.P. Ghatak, Physica E **36**, 163 (2007); K.P. Ghatak, S. Bhattacharya, S. Bhowmik, R. Benedictus, S. Choudhury, J. Appl. Phys. **103**, 1 (2008); M. Mondal, A. Ghoshal, K.P. Ghatak, Nouvo Cimento D **14D**, 63 (1992); K.P. Ghatak, Nouvo Cimento D **13D**, 1321 (1992); K.P. Ghatak, M. Mondal, J. Appl. Phys.

**70**, 299 (1991); K.P. Ghatak, S.N. Biswas, J. Low Temp. Phys. **78**, 219 (1990); K.P. Ghatak, M. Mondal, J. Appl. Phys. **65**, 3480 (1989); J. Appl. Phys. **66**, 3056 (1989)

53. K.P. Ghatak, B. De, M. Modal, S.N. Biswas, Epitaxial Hetrostructures, MRS Symposium Proceedings Spring Meeting **198**, 327 (1990); K.P. Ghatak, S.N. Biswas, Long Wave Length Semiconductor Devices, Materials and Processes MRS Symposium Proceedings, MRS Spring Meeting **216**, 465 (1990); K.P. Ghatak, B. De, Modern Perspective on Thermoelectrics and Related Materials, MRS Symposium Proceedings, Spring Meeting **234**, 55 (1991); K.P. Ghatak, B. De, Modern Perspective on Thermoelectrics and Related Materials, MRS Symposium Proceedings, Spring Meeting **234**, 59 (1991); K.P. Ghatak, Proceedings of SPIE, USA, Fiber Optic and Laser Sensors IX **1584**, 435 (1992)
54. R.B. Dingle, Phil Mag **46**, 813 (1955); D. Redfield, M.A. Afromowitz, Phil. Mag. **18,** 831 (1969); H.C. Cassey, F. Stern, J. Appl. Phys. **47**, 631 (1976); M. Mondal, K.P. Ghatak, Physics Lett. **102A**, 54 (1984); P.K. Chakraborty, G.C. Datta, K.P. Ghatak, Physica Scripta **68**, 368 (2003); B. Mitra, D.K. Basu, B. Nag, K.P. Ghatak, Nonlinear Opt. **17**, 171 (1997); K.P. Ghatak, S. Bhattacharya, J. Appl. Phys. **102**, 073704 (2007)
55. K.P. Ghatak, S. Bhattacharya, H. Saikia, D. Baruah, A. Saikia, K.M. Singh, A. Ali, S.N. Mitra, P.K. Bose, A. Sinha, J. Comput. Theor. Nanosci. **3**, 727 (2006)
56. E.O. Kane, Solid State Electron. **8**, 3 (1985); T. Ando, A.H. Fowler, F. Stern, Rev. Modern Phys. **54**, 437 (1982); P.K. Basu, *Optical Processes in Semiconductors.* (Oxford University Press, 2001); A.N. Chakravarti, D. Mukherjee, Phys. Lett. **53A**, 403 (1975); A.N. Chakravarti, S. Swaminathan, Phys. Stat. Sol. (a) **23**, K191 (1974); A.N. Chakravarti, Phys. Stat. Sol. (a) **25**, K 105 (1974)
57. A.K. Sreedhar, S.C. Gupta, Phys. Rev. B **5**, 3160 (1972); R.W. Keyes, IBM. J. Res. Develop. **5**, 266 (1961); R.W. Keyes, Solid State Phys. **20**, 37 (1967)
58. S. Bhattacharya, S. Chowdhury, K.P. Ghatak, J. Comput. Theor. Nanosci. **3**, 423 (2006); S. Choudhury, L.J. Singh, K.P. Ghatak, Physica B **365**, 5 (2005); L.J. Singh, S. Choudhary, A. Mallik, K.P. Ghatak, J. Comput. Theor. Nanosci. **2**, 287 (2005); K. P. Ghatak, J.Y. Siddiqui, B. Nag, Phys. Lett. A **282**, 428 document (2001); K.P. Ghatak, J.P. Banerjee, B. Nag, J. Appl. Phys. **83**, 1420 (1998); B. Nag, K.P. Ghatak, Nonlin. Opt. **19**, 1 (1998); K.P. Ghatak, B. Nag, Nanostruct. Mater. **10**, 923 (1998); B. Nag, K.P. Ghatak, J. Phys. Chem. Sol. **58**, 427 (1997)
59. K.P. Ghatak, D.K. Basu, B. Nag, J. Phys. Chem. Sol. **58**, 133 (1997); K.P. Ghatak, J.P. Banerjee, B. Goswami, B. Nag, Nonlin. Opt. Quant. Opt. **16**, 241 (1996); K.P. Ghatak, J.P. Banerjee, D. Bhattacharyya, B. Nag, Nanotechnology **7**, 110 (1996); K. P. Ghatak, J.P. Banerjee, M. Mitra, B. Nag, Nonlin. Opt. **17**, 193 (1996); B. Nag, K. P. Ghatak, Phys. Scr. **54**, 657 (1996); K.P. Ghatak, B. Mitra, Phys. Scr. **46**, 182 (1992); K.P. Ghatak, Int. J. Electron. **71**, 239 (1991)
60. K.P. Ghatak, B. De, S.N. Biswas, M. Mondal, Mechanical Behavior of Materials and Structures in Microelectronics, MRS Symposium Proceedings, Spring Meeting **2216**,191 (1991); K.P. Ghatak, B. De, MRS Symposium Proceedings **226**, 191 (1991); K.P. Ghatak, B. Nag, G. Majumdar, Proceedings of MRS **379**, 109 (1995); D. Baruah, S. Choudhury, K.M. Singh, K.P. Ghatak, J. Phys. Conf. Series **61**, 80 (2007)

# 2

# The Einstein Relation in Bulk Specimens of Compound Semiconductors

## 2.1 Investigation on Tetragonal Materials

### 2.1.1 Introduction

It is well known that the $A_{III}^2 B_{II}^5$ and the ternary chalcopyrite compounds are called tetragonal materials due to their tetragonal crystal structures [1]. These materials find extensive use in non-linear optical elements [2], photodetectors [3] and light emitting diodes [4]. Rowe and Shay [5] showed that the quasi-cubic model [6] can be used to explain the observed splitting and symmetry properties of the band structure at the zone center of **k** space of the aforementioned materials. The s-like conduction band is singly degenerate and the p-like valence bands are triply degenerate. The latter splits into three subbands because of the spin–orbit and the crystal field interactions. The largest contribution to the crystal field splitting is from the non-cubic potential [7]. The experimental results on the absorption constants, the effective mass, and the optical third order susceptibility indicate that the fact that the conduction band in the same materials corresponds to a single ellipsoidal revolution at the zone center in k-space [1, 8]. Introducing the crystal potential in the Hamiltonian, Bodnar [9] derived the electron dispersion relation in the same material under the assumption of an isotropic spin–orbit splitting constant. It would, therefore, be of much interest to investigate the DMR in these compounds by including the anisotropies of the spin–orbit splitting constant and, the effective electron mass together with the inclusion of crystal field splitting, within the framework of **k.p** formalism since, these are the important physical features of such materials [1].

In what follows, in Sect. 2.1.2 on the theoretical background the expressions for the electron concentration and the DMR for tetragonal compounds have been derived on the basis of the generalized dispersion relation. In Sect. 2.1.3, it has been shown that the corresponding results for III–V, ternary and quaternary materials form special cases of our generalized analysis. The expressions for $n_0$ and DMR for semiconductors whose energy band structures are defined by the two-band model of Kane and that of parabolic energy bands have further been formulated under certain constraints. For the purpose of numerical computations, n-$Cd_3As_2$ and n-$CdGeAs_2$ have been used as examples of $A_{III}^2B_{II}^5$ and the ternary chalcopyrite compounds, which are being extensively used in Hall pick-ups, thermal detectors, and non-linear optics [3]. In addition, the DMR has also been numerically investigated by taking n-InAs and n-InSb as examples of III–V semiconductors, n-$Hg_{1-x}Cd_xTe$ as an example of ternary compounds and n-$In_{1-x}Ga_xAs_yP_{1-y}$ lattice matched to InP as example of quaternary materials in accordance with the three and the two band models of Kane together with parabolic energy bands, respectively, for the purpose of relative comparison. The importance of the aforementioned materials in electronics has been discussed in Sect. 2.1.3. Section 2.1.4 contains the results and discussions.

### 2.1.2 Theoretical Background

The form of **k.p** matrix for tetragonal semiconductors can be expressed, extending Bodnar's [9] relation, as

$$H = \begin{bmatrix} H_1 & H_2 \\ H_2{}^{+} & H_1 \end{bmatrix}, \tag{2.1}$$

where $H_1 \equiv \begin{bmatrix} E_g & 0 & P_{||}k_z & 0 \\ 0 & \left(-2\Delta_{||}/3\right) & \left(\sqrt{2}\Delta_{\perp}/3\right) & 0 \\ P_{||}k_z & \left(\sqrt{2}\Delta_{\perp}/3\right) & -\left(\delta + \frac{1}{3}\Delta_{||}\right) & 0 \\ 0 & 0 & 0 & 0 \end{bmatrix}$ and $H_2 \equiv \begin{bmatrix} 0 & -f_{,+} & 0 & f_{,-} \\ f_{,+} & 0 & 0 & 0 \\ 0 & 0 & 0 & 0 \\ f_{,+} & 0 & 0 & 0 \end{bmatrix}$,

in which $E_g$ is the band gap, $P_{||}$ and $P_{\perp}$ are the momentum matrix elements parallel and perpendicular to the direction of crystal axis respectively, $\delta$ is the crystal field splitting constant, $\Delta_{||}$ and $\Delta_{\perp}$ are the spin–orbit splitting constants parallel and perpendicular to the $C$-axis respectively, $f_{,\pm} \equiv \left(P_{\perp}/\sqrt{2}\right)\left(k_x \pm \mathrm{i}k_y\right)$ and $i = \sqrt{-1}$. Thus, neglecting the contribution of the higher bands and the free electron term, the diagonalization of the above matrix leads to the dispersion relation of the conduction electrons in bulk specimens of tetragonal compounds [1] as

$$\psi_1(E) = \psi_2(E)\,k_s^2 + \psi_3(E)\,k_z^2, \tag{2.2}$$

where

$$\psi_1(E) \equiv E(E+E_g)\left[\left(E+E_g\right)\left(E+E_g+\Delta_{||}\right) + \delta\left(E+E_g+\frac{2}{3}\Delta_{||}\right) + \frac{2}{9}\left(\Delta_{||}^2 - \Delta_{\perp}^2\right)\right],\ k_s{}^2 = k_x{}^2 + k_y{}^2,$$

$$\psi_2(E) \equiv \frac{\hbar^2 E_{\mathrm{g}}\left(E_{\mathrm{g}}+\Delta_{\perp}\right)}{\left[2m_{\perp}^{*}\left(E_{\mathrm{g}}+\frac{2}{3}\Delta_{\perp}\right)\right]}\left[\delta\left(E+E_{\mathrm{g}}+\frac{1}{3}\Delta_{||}\right)+\left(E+E_{\mathrm{g}}\right)\right.$$
$$\left.\times\left(E+E_{\mathrm{g}}+\frac{2}{3}\Delta_{||}\right)+\frac{1}{9}\left(\Delta_{||}^{2}-\Delta_{||}^{2}\right)\right],$$

$\psi_3(E) \equiv \frac{\hbar^2 E_{\mathrm{g}}\left(E_{\mathrm{g}}+\Delta_{||}\right)}{\left[2m_{||}^{*}\left(E_{\mathrm{g}}+\frac{2}{3}\Delta_{||}\right)\right]}\left[\left(E+E_{\mathrm{g}}\right)\left(E+E_{\mathrm{g}}+\frac{2}{3}\Delta_{||}\right)\right]$, $m_{||}^{*}$ and $m_{\perp}^{*}$ are the longitudinal and transverse effective electron masses at the edge of the conduction band respectively.

The general expression of the density-of-states (DOS) function in bulk semiconductors is given by

$$D_0(E) = \frac{2g_{\mathrm{v}}}{(2\pi)^3}\left(\frac{\partial}{\partial E}\left[V(E)\right]\right), \tag{2.3a}$$

where $g_{\mathrm{v}}$ is the valley degeneracy and $V(E)$ is the volume of $\mathbf{k}$ space. Using (2.2) and (2.3a), we get

$$D_0(E) = g_{\mathrm{v}}\left(3\pi^2\right)^{-1}\psi_4(E), \tag{2.3b}$$

$$\psi_4(E) \equiv \left[\frac{3}{2}\frac{\sqrt{\psi_1(E)}\left[\psi_1(E)\right]'}{\psi_2(E)\sqrt{\psi_3(E)}}-\frac{\left[\psi_2(E)\right]'\left[\psi_1(E)\right]^{3/2}}{\left[\psi_2(E)\right]^2\sqrt{\psi_3(E)}}\right.$$
$$\left.-\frac{1}{2}\frac{\left[\psi_3(E)\right]'\left[\psi_1(E)\right]^{3/2}}{\psi_2(E)\left[\psi_3(E)\right]^{3/2}}\right],$$
$$\left[\psi_1(E)\right]' \equiv \left[\,\left(2E+E_{\mathrm{g}}\right)\psi_1(E)\left[E\left(E+E_{\mathrm{g}}\right)\right]^{-1}+E(E+E_{\mathrm{g}})\right.$$
$$\left.\times\left(2E+2E_{\mathrm{g}}+\delta+\Delta_{||}\right)\,\right],$$
$$\left[\psi_2(E)\right]' \equiv \left[2m_{\perp}^{*}\left(E_{\mathrm{g}}+\frac{2}{3}\Delta_{\perp}\right)\right]^{-1}\left[\hbar^2 E_{\mathrm{g}}\left(E_{\mathrm{g}}+\Delta_{\perp}\right)\right]$$
$$\times\left[\delta+2E+2E_{\mathrm{g}}+\frac{2}{3}\Delta_{||}\right],$$

and $\left[\psi_3(E)\right]' \equiv \left[2m_{||}^{*}\left(E_{\mathrm{g}}+\frac{2}{3}\Delta_{||}\right)\right]^{-1}\left[\hbar^2 E_{\mathrm{g}}\left(E_{\mathrm{g}}+\Delta_{||}\right)\right]\left[2E+2E_{\mathrm{g}}+\frac{2}{3}\Delta_{||}\right]$, in which, the primes denote the differentiation of the differentiable functions with respect to $E$.

Combining (2.3b) with the Fermi–Dirac occupation probability factor and using the generalized Sommerfeld's lemma [10], the electron concentration can be written as

$$n_0 = g_{\mathrm{v}}\left(3\pi^2\right)^{-1}\left[M\left(E_{\mathrm{F}}\right)+N\left(E_{\mathrm{F}}\right)\right], \tag{2.4}$$

where $M(E_{\mathrm{F}}) \equiv \left[\frac{\left[\psi_1(E_{\mathrm{F}})\right]^{\frac{3}{2}}}{\psi_2(E_{\mathrm{F}})\sqrt{\psi_3(E_{\mathrm{F}})}}\right]$, $E_{\mathrm{F}}$ is the Fermi energy as measured from the edge of the conduction band in the vertically upward direction in the absence of any quantization, $N(E_{\mathrm{F}}) \equiv \sum_{r=1}^{s} L(r)M(E_{\mathrm{F}})$, $r$ is the set of real positive integers whose upper limit is $s$, $L(r) \equiv \left[2\left(k_{\mathrm{B}}T\right)^{2r}\left(1-2^{1-2r}\right)\xi\left(2r\right)\right] \times \left[\frac{\partial^{2r}}{\partial E_{\mathrm{F}}^{2r}}\right]$ and $\zeta(2r)$ is the Zeta function of order $2r$ [11].

Thus the use of the (2.4) and (1.11) leads to the expression of DMR as

$$\frac{D}{\mu} = \frac{1}{|e|}\frac{\left[M\left(E_{\mathrm{F}}\right)+N\left(E_{\mathrm{F}}\right)\right]}{\left[\left\{M\left(E_{\mathrm{F}}\right)\right\}'+\left\{N\left(E_{\mathrm{F}}\right)\right\}'\right]}. \tag{2.5}$$

### 2.1.3 Special Cases for III–V Semiconductors

(a) Under the substitutions $\delta = 0, \Delta_{||} = \Delta_{\perp} = \Delta$(the isotropic spin–orbit splitting constant) and $m_{||}^{*} = m_{\perp}^{*} = m^{*}$(the isotropic effective electron mass at the edge of the conduction band), (2.2) assumes the form [1]

$$\frac{\hbar^2 k^2}{2m^*} = \gamma(E),\ \ \gamma(E) \equiv \frac{E(E+E_{\mathrm{g}})(E+E_{\mathrm{g}}+\Delta)\left(E_{\mathrm{g}}+\frac{2}{3}\Delta\right)}{E_{\mathrm{g}}(E_{\mathrm{g}}+\Delta)\left(E+E_{\mathrm{g}}+\frac{2}{3}\Delta\right)}, \tag{2.6}$$

which is the well-known three band model of Kane [1]. Equation (2.6) is the dispersion relation of the conduction electrons of III–V, ternary and quaternary materials and should be used as such for studying the electron transport in n-InAs where the spin orbit splitting constant is of the order of band gap. The III–V compounds are used in integrated optoelectronics [12, 13], passive filter devices [14], distributed feedback lasers and Bragg reflectors [15]. Besides, we shall also use n-$\mathrm{Hg}_{1-x}\mathrm{Cd}_x\mathrm{Te}$ and n-$\mathrm{In}_{1-x}\mathrm{Ga}_x\mathrm{As}_y\mathrm{P}_{1-y}$ lattice matched to InP as examples of ternary and quaternary materials respectively. The ternary alloy n-$\mathrm{Hg}_{1-x}\mathrm{Cd}_x\mathrm{Te}$ is a classic narrow-gap compound and is technologically an important optoelectronic semiconductor because its band gap can be varied to cover a spectral range from 0.8 to over 30 μm by adjusting the alloy composition [16]. The n-$\mathrm{Hg}_{1-x}\mathrm{Cd}_x\mathrm{Te}$ finds applications in infrared detector materials [17] and photovoltaic detector [18] arrays in the 8-12 μm wave bands. The above applications have spurred an $\mathrm{Hg}_{1-x}\mathrm{Cd}_x\mathrm{Te}$ technology for the production of high mobility single crystals, with specially prepared surface layers and the same material is suitable for narrow subband physics because the relevant material constants are within experimental reach [19]. The quaternary compounds are being extensively used in optoelectronics, infrared light emitting diodes, high electron mobility transistors, visible heterostructure lasers for fiber optic systems, semiconductor lasers, [20], tandem solar cells [21], avalanche photodetectors [22], long wavelength light sources, detectors in optical fiber communications, [23] and new types of optical devices, which are being prepared from the quaternary systems [24].

Under the aforementioned limiting conditions, the density-of-states function, the electron concentration, and the DMR in accordance with the three band model of Kane assume the following forms

$$D_0(E) = 4\pi g_{\mathrm{v}} \left(\frac{2m^*}{h^2}\right)^{3/2} \sqrt{\gamma(E)}\,[\gamma_1(E)], \tag{2.7}$$

$$n_0 = \frac{g_{\mathrm{v}}}{3\pi^2}\left(\frac{2m^*}{\hbar^2}\right)^{3/2} [M_1(E_{\mathrm{F}}) + N_1(E_{\mathrm{F}})], \tag{2.8}$$

and

$$\frac{D}{\mu} = \frac{1}{|e|}[M_1(E_{\mathrm{F}}) + N_1(E_{\mathrm{F}})]\left[\{M_1(E_{\mathrm{F}})\}' + \{N_1(E_{\mathrm{F}})\}'\right]^{-1}, \tag{2.9}$$

where $\gamma_1(E) \equiv \gamma(E)\left[\frac{1}{E} + \frac{1}{E+E_{\mathrm{g}}} + \frac{1}{E+E_{\mathrm{g}}+\Delta} - \frac{1}{E+E_{\mathrm{g}}+\frac{2}{3}\Delta}\right]$, $M_1(E_{\mathrm{F}}) \equiv [\gamma(E_{\mathrm{F}})]^{3/2}$ and $N_1(E_{\mathrm{F}}) \equiv \sum\limits_{r=1}^{s} L(r)\,M_1(E_{\mathrm{F}})$.

(b) Under the inequalities $\Delta \gg E_{\mathrm{g}}$ or $\Delta \ll E_{\mathrm{g}}$, (2.6) gets simplified as [1]

$$\frac{\hbar^2 k^2}{2m^*} = E(1+\alpha E), \quad \alpha \equiv 1/E_{\mathrm{g}}, \tag{2.10}$$

which is known as the two-band model of Kane [1]. Under the above constraints, the forms of the DOS, the electron statistics and the DMR can, respectively, be written as,

$$D_0(E) = 4\pi g_{\mathrm{v}} \left(\frac{2m^*}{h^2}\right)^{3/2} \sqrt{I(E)}\,[I_1(E)], \tag{2.11}$$

$$n_0 = \frac{g_{\mathrm{v}}}{3\pi^2}\left(\frac{2m^*}{\hbar^2}\right)^{3/2} [M_2(E_{\mathrm{F}}) + N_2(E_{\mathrm{F}})], \tag{2.12}$$

and

$$\frac{D}{\mu} = \frac{1}{|e|}[M_2(E_{\mathrm{F}}) + N_2(E_{\mathrm{F}})]\left[\{M_2(E_{\mathrm{F}})\}' + \{N_2(E_{\mathrm{F}})\}'\right]^{-1}, \tag{2.13}$$

where $I(E) \equiv E(1+\alpha E)$, $I_1(E) \equiv (1+2\alpha E)$, $M_2(E_{\mathrm{F}}) \equiv [I(E_{\mathrm{F}})]^{3/2}$ and $N_2(E_{\mathrm{F}}) \equiv \sum\limits_{r=1}^{s} L(r)\,M_2(E_{\mathrm{F}})$.

(c) Under the constraints $\Delta \gg E_{\mathrm{g}}$ or $\Delta \ll E_{\mathrm{g}}$ together with the inequality $\alpha E_{\mathrm{F}} \ll 1$, we can write [1]

$$n_0 = g_{\mathrm{v}} N_{\mathrm{c}}\left[F_{1/2}(\eta) + \left(\frac{15\alpha k_{\mathrm{B}}T}{4}\right)F_{3/2}(\eta)\right], \tag{2.14}$$

$$\text{and } \frac{D}{\mu} = \left[\frac{k_{\mathrm{B}}T}{|e|}\right]\left[\frac{\left(F_{1/2}(\eta) + \left(\frac{15\alpha k_{\mathrm{B}}T}{4}\right)F_{3/2}(\eta)\right)}{\left(F_{-1/2}(\eta) + \left(\frac{15\alpha k_{\mathrm{B}}T}{4}\right)F_{1/2}(\eta)\right)}\right], \tag{2.15}$$

where $N_{\mathrm{C}} \equiv 2\left(\frac{2\pi m^{*} k_{\mathrm{B}} T}{h^{2}}\right)^{3/2}$ $\eta \equiv \frac{E_{\mathrm{F}}}{k_{\mathrm{B}} T}$ and $F_j(\eta)$ is the one parameter Fermi–Dirac integral of order $j$ which can be written as [25],

$$F_j(\eta) = \left(\frac{1}{\Gamma(j+1)}\right) \int\limits_0^{\infty} y^j \left(1 + \exp(y - \eta)\right)^{-1} \mathrm{d}y, \quad j > -1, \tag{2.16}$$

where $\Gamma(j+1)$ is the complete Gamma function or for all $j$, analytically continued as a complex contour integral around the negative axis

$$F_j(\eta) = A_j \int\limits_{-\infty}^{(0+)} y^j \left(1 + \exp(-y - \eta)\right)^{-1} \mathrm{d}y, \tag{2.17}$$

in which $A_j \equiv \frac{\Gamma(-j)}{2\pi\sqrt{-1}}$.

(d) For relatively wide gap materials $E_{\mathrm{g}} \to \infty$ and (2.14) and (2.15) assume the forms

$$n_0 = g_{\mathrm{v}} N_{\mathrm{c}} F_{1/2}(\eta) \tag{2.18}$$

and

$$\frac{D}{\mu} = \left(\frac{k_{\mathrm{B}} T}{|e|}\right) \left[\frac{F_{1/2}(\eta)}{F_{-1/2}(\eta)}\right]. \tag{2.19}$$

Equation (2.19) was derived for the first time by Landsberg [1].

(e) Combining (2.18) and (2.19) and using the formula $\frac{\mathrm{d}}{\mathrm{d}\eta}[F_j(\eta)] = F_{j-1}(\eta)$ [25] as easily derived from (2.16) and (2.17) together with the fact that under the condition of extreme carrier degeneracy

$$F_{1/2}(\eta) = \left[\frac{4}{3\sqrt{\pi}}\right] (\eta)^{3/2}, \tag{2.20}$$

we can write

$$n_0 = \frac{g_{\mathrm{v}}}{3\pi^2} \left[\frac{2m^{*} E_{\mathrm{F}}(1 + \alpha E_{\mathrm{F}})}{\hbar^2}\right]^{3/2}, \tag{2.21}$$

and

$$\frac{D}{\mu} = \frac{1}{|e|} \left(\frac{2}{3}\right) E_{\mathrm{F}} \frac{(1 + \alpha E_{\mathrm{F}})}{(1 + 2\alpha E_{\mathrm{F}})}, \tag{2.22}$$

For $\alpha \to 0$, (2.21) and (2.22) assume the forms

$$n_0 = \frac{g_{\mathrm{v}}}{3\pi^2} \left[\frac{2m^{*} E_{\mathrm{F}}}{\hbar^2}\right]^{3/2}, \tag{2.23}$$

and

$$\frac{D}{\mu} = \frac{2E_{\mathrm{F}}}{3|e|}. \tag{2.24}$$

(f) Under the condition of non-degenerate electron concentration $\eta \ll 0$ and $F_j(\eta) \cong \exp(\eta)$ for all $j$ [25]. Therefore (2.18) and (2.19) assume the well-known forms as [1]

$$n_0 = g_{\mathrm{v}} N_{\mathrm{c}} \exp(\eta), \tag{2.25}$$

and

$$\frac{D}{\mu} = \frac{k_{\mathrm{B}} T}{|e|}. \tag{2.26}$$

### 2.1.4 Result and Discussions

Using n-$\mathrm{Cd_3As_2}$ as an example of $A_{III}^2 B_{II}^5$ compounds for the purpose of numerical computations and using (2.4) and (2.5) together with the energy band constants at $T = 4.2\,\mathrm{K}$, as given in Table 2.1, the variation of the DMR as a function of electron concentration has been shown in curve (a) of Fig. 2.1. The circular points exhibit the same dependence and have been obtained by using (1.15) and taking the experimental values of the thermoelectric power in $n{-}\mathrm{Cd_3As_2}$ in the presence of a classically large magnetic field [26]. The curve (b) corresponds to $\delta = 0$. The curve (c) shows the dependence of the DMR on $n_0$ in accordance with the three-band model of Kane using the energy band constants as $E_{\mathrm{g}} = 0.095\,\mathrm{eV}$, $m^* = \left(m_{||}^* + m_{\perp}^*\right) / 2$ and $\Delta = \left(\Delta_{||} + \Delta_{\perp}\right) / 2$. The curves (d) and (e) correspond to the two-band model of Kane and that of the parabolic energy bands. By comparing the curves (a) and (b) of Fig. 2.1, one can easily assess the influence of crystal field splitting on the DMR in tetragonal compounds. Figure 2.2 represents all cases of Fig. 2.1 for n-$\mathrm{CdGeAs_2}$ which has been used as an example of ternary chalcopyrite materials where the values of the energy band constants of the said compound are given in Table 2.1.

It appears from Fig. 2.1 that, the DMR in tetragonal compounds increases with increasing carrier degeneracy as expected for degenerate semiconductors and agrees well with the suggested experimental method of determining the same ratio for materials having arbitrary carrier energy spectra. It has been observed that the tetragonal crystal field affects the DMR of the electrons quite significantly in this case. The dependence of the DMR is directly determined by the band structure because of its immediate connection with the Fermi energy. The DMR increases non-linearly with the electron concentration in other limiting cases and the rates of increase are different from that in the generalized band model.

From Fig. 2.2, one can assess that the DMR in bulk specimens of n-$\mathrm{CdGeAs_2}$ exhibits monotonic increasing dependence with increasing electron concentration. The cases (b), (c) and (d) of Fig. 2.2 for n-$\mathrm{CdGeAs_2}$ exhibit the similar trends with change in the respective numerical values of the DMR. The influence of spectrum constants on the DMR for n-$\mathrm{Cd_3As_2}$ and n-$\mathrm{CdGeAs_2}$ can also be assessed by comparing the respective variations as drawn in Figs. 2.1 and 2.2 respectively.

**Table 2.1.** The numerical values of the energy band constants of few materials

| Materials | |
|---|---|
| $n-Cd_3As_2$ | $\lvert E_g \rvert = 0.095\,\mathrm{eV}$, $\Delta_{\parallel} = 0.27\,\mathrm{eV}$, $\Delta_\perp = 0.25\,\mathrm{eV}$, $m^*_{\parallel} = 0.00697m_0$ ($m_0$ is the free electron mass), $m^*_\perp = 0.013933m_0$, $\delta = 0.085\mathrm{eV}$, $g_v = 1$ [25,73] and $\varepsilon_{sc} = 16\varepsilon_0$ ($\varepsilon_{sc}$ and $\varepsilon_0$ are the permittivity of the semiconductor and free space respectively) [74] |
| $n-CdGeAs_2$ | $E_g = 0.57\,\mathrm{eV}$, $\Delta_{\parallel} = 0.30\,\mathrm{eV}$, $\Delta_\perp = 0.36\,\mathrm{eV}$, $m^*_{\parallel} = 0.034m_o$, $m^*_\perp = 0.039m_o$, $T = 4\,\mathrm{K}$, $\delta = -0.21\,\mathrm{eV}$, $g_v = 1$ [1,26] and $\varepsilon_{sc} = 18.4\varepsilon_0$ [75] |
| n-InAs | $E_g = 0.36\,\mathrm{eV}$, $\Delta = 0.43\,\mathrm{eV}$ and $m^* = 0.026m_0$, $g_v = 1$, $\varepsilon_{sc} = 12.25\varepsilon_0$ [76] |
| n-InSb | $E_g = 0.2352\,\mathrm{eV}$, $\Delta = 0.81\,\mathrm{eV}$ and $m^* = 0.01359m_0$, $g_v = 1$, $\varepsilon_{sc} = 15.56\varepsilon_0$ [76] |
| $n-Ga_{1-x}Al_xAs$ | $E_g(x) = (1.424 + 1.266x + 0.26x^2)\mathrm{eV}$, $\Delta(x) = (0.34 - 0.5x)\mathrm{eV}$, $m^*(x) = [0.066 + 0.088x]\,m_0$ $g_v = 1$, $\varepsilon_{sc}(x) = [13.18 - 3.12x]\,\varepsilon_0$ [77] |
| $Hg_{1-x}Cd_xTe$ | $E_g(x) = \left(-0.302 + 1.93x + 5.35\times10^{-4}(1-2x)T - 0.810x^2 + 0.832x^3\right)\,\mathrm{eV}$, $\Delta(x) = \left(0.63 + 0.24x - 0.27x^2\right)\,\mathrm{eV}$, $m^* = 0.1m_0E_g(\mathrm{eV})^{-1}$, $g_v = 1$ and $\varepsilon_{sc} = \left[20.262 - 14.812x + 5.22795x^2\right]\varepsilon_0$ [78] |
| $In_{1-x}Ga_xAs_yP_{1-y}$ lattice matched to InP | $E_g = \left(1.337 - 0.73y + 0.13y^2\right)\,\mathrm{eV}$, $\Delta = \left(0.114 + 0.26y - 0.22y^2\right)\,\mathrm{eV}$, $m^* = (0.08 - 0.039y)\,m_o$, $y = (0.1896 - 0.4052x)(0.1896 - 0.0123x)^{-1}$, $g_v = 1$ [79] and $\varepsilon_{sc} = [10.65 + 0.1320y]\,\varepsilon_0$ [80] |
| *CdS* | $m^*_{\parallel} = 0.7m_o$, $m^*_\perp = 1.5m_o$ and $\bar{\lambda}_0 = 1.4\times10^{-10}\,\mathrm{eVm}$, $g_v = 1$ [76] and $\varepsilon_{sc} = 15.5\varepsilon_0$ [81] |
| n-PbTe | $m_t^- = 0.070m_0$, $m_l^- = 0.54m_0$, $m_t^+ = 0.010m_0$, $m_l^+ = 1.4m_0$, $P_{\parallel} = 141\,\mathrm{meV\,nm}$, $P_\perp = 486\,\mathrm{meV\,nm}$, $E_g = 190\,\mathrm{meV}$, $g_v = 4$ [12] and $\varepsilon_{sc} = 33\varepsilon_0$ [76,82] |
| n-PbSnTe | $m_t^- = 0.063m_0$, $m_l^- = 0.41m_0$, $m_t^+ = 0.089m_0$, $m_l^+ = 1.6m_0$, $P_{\parallel} = 137\,\mathrm{meV\,nm}$, $P_\perp = 464\,\mathrm{meV\,nm}$, $E_g = 90\,\mathrm{meV}$, $g_v = 4$ [12] and $\varepsilon_{sc} = 60\varepsilon_0$ [76,82] |
| $n-Pb_{1-x}Sn_xSe$ | $x = 0.31$, $g_v = 4$, $m_t^- = 0.143m_0$, $m_l^- = 2.0m_0$, $m_t^+ = 0.167m_0$, $m_l^+ = 0.286m_0$, $P_{\parallel} = 3.2\times10^{-10}\,\mathrm{eVm}$, $P_\perp = 4.1\times10^{-10}\,\mathrm{eVm}$, $E_g = 0.137\mathrm{eV}$, $g_v = 4$ [12] and $\varepsilon_{sc} = 31\varepsilon_0$ [76,83] |
| Stressed n-InSb | $m^* = 0.048m_o$, $E_g = 0.081\,\mathrm{eV}$, $B_2 = 9\times10^{-10}\,\mathrm{eVm}$, $C_1^c = 3\,\mathrm{eV}$, $C_2^c = 2\,\mathrm{eV}$, $a_0 = -10\,\mathrm{eV}$, $b_0 = -1.7\,\mathrm{eV}$, $d_0 = -4.4\,\mathrm{eV}$, $S_{xx} = 0.6\times10^{-3}\,(\mathrm{kbar})^{-1}$, $S_{yy} = 0.42\times10^{-3}\,(\mathrm{kbar})^{-1}$, $S_{zz} = 0.39\times10^{-3}\,(\mathrm{kbar})^{-1}$ and $S_{xy} = 0.5\times10^{-3}\,(\mathrm{kbar})^{-1}$, $\varepsilon_{xx} = \sigma S_{xx}$, $\varepsilon_{yy} = \sigma S_{yy}$, $\varepsilon_{zz} = \sigma S_{zz}$, $\varepsilon_{xy} = \sigma S_{xy}$ and $\sigma$ is the stress in kilobar, $g_v = 1$ [44] |

(*Continued*)

**Table 2.1.** *Continued*

| | |
|---|---|
| $PtSb_2$ | For conduction bands, along <111> direction, $\lambda_1 = 0.33\,\mathrm{eV}$, $l_1 = 1.09\,\mathrm{eV}$, $\nu_1 = 0.17\,\mathrm{eV}$, $n_1 = 0.22\,\mathrm{eV}$, $a = 0.643\,\mathrm{nm}$, $I_0 = 0.30\ (\mathrm{eV})^2$, $\delta_0' = 0.33\,\mathrm{eV}$, $g_v = 8$ [56] and $\varepsilon_{sc} = 30\varepsilon_0$ [56, 84] |
| n-GaSb | $E_g = 0.81\,\mathrm{eV}$, $\Delta = 0.80\,\mathrm{eV}$, $P = 9.48 \times 10^{-10}\,\mathrm{eVm}$, $\bar{\varsigma}_0 = -2.1$, $\bar{v}_0 = -1.49$, $\bar{\omega}_0 = 0.42$, $g_v = 1$ [53] and $\varepsilon_{sc} = 15.85\varepsilon_0$ [53, 85] |
| HgTe | $m_v^* = 0.028 m_0$, $g_v = 1$ and $\varepsilon_\infty = 15.2\varepsilon_0$ [52] |
| Bismuth | $E_g = 0.0153\,\mathrm{eV}$, $m_1 = 0.00194 m_0$, $m_2 = 0.313 m_0$, $m_3 = 0.00246 m_0$, $m_2' = 0.36 m_0$, $g_v = 3$ and $g_s = 2$ [42] |

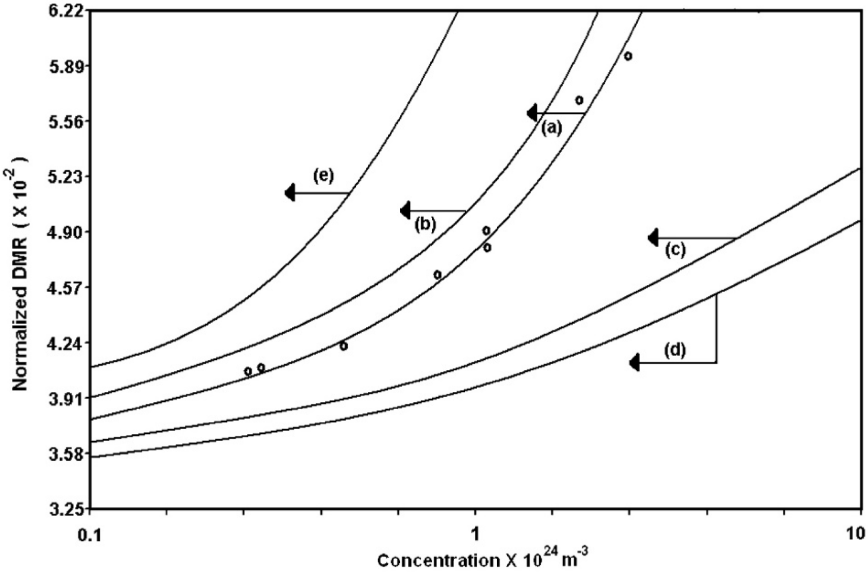

**Fig. 2.1.** The plot of the DMR in the bulk specimens of n-$Cd_3As_2$ as a function of electron concentration in accordance with (**a**) the generalized band model; (**b**) $\delta = 0$; (**c**) the three band model of Kane; (**d**) the two band model of Kane and (**e**) the parabolic energy bands. The *dotted circular points* show the same dependence which have been obtained by using (1.15) and taking the experimental values of the thermoelectric power of the electrons in bulk n-$Cd_3As_2$ in the presence of a classically large magnetic field [26]

Using the appropriate equations, one can numerically evaluate the DMR as a function of electron concentration for n-InAs, whose energy band constants are presented in Table 2.1. This is shown in Fig. 2.3 by curves (a), (b) and (c) respectively, in accordance with the three and two band models of Kane together with the model of parabolic energy bands. Figure 2.4 exhibits all the cases of Fig. 2.3 for n-InSb whose energy band constants are given in Table 2.1.

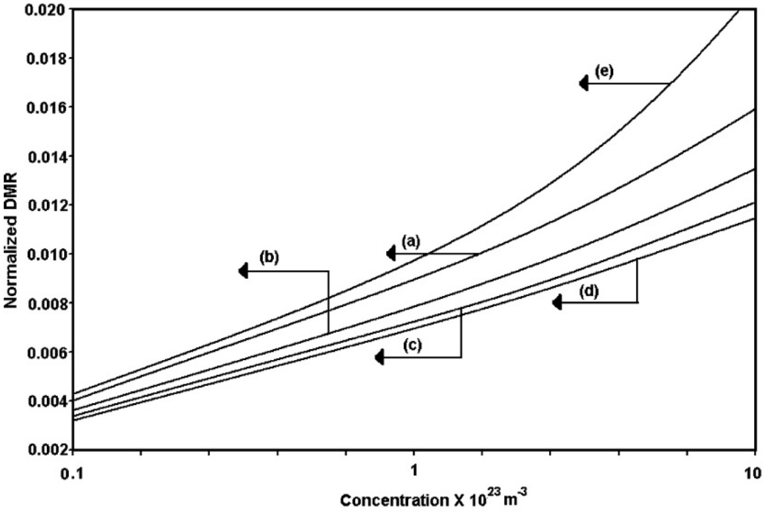

**Fig. 2.2.** The plot of the DMR in the bulk specimens of n-$CdGeAs_2$ as a function of electron concentration in accordance with (**a**) the generalized band model; (**b**) $\delta = 0$; (**c**) the three band model of Kane; (**d**) the two band model of Kane and (**e**) the parabolic energy bands

From Figs. 2.3 and 2.4 one can observe that the numerical values of the DMR for n-InAs and n-InSb in accordance with the three band model of Kane are less than that of the corresponding parabolic energy bands for relatively large values of the electron concentration. Also, the numerical values of the DMR in accordance with two-band model of Kane also changes as compared with the corresponding three-band model of Kane for n-InAs. The influence of energy band constants on the DMR for n-InAs and n-InSb becomes apparent by comparing Figs. 2.3 and 2.4 respectively.

For n-$Hg_{1-x}Cd_xTe$ together with the numerical values of the spectrum constants as given in Table 2.1, the DMR has been plotted at $T = 4.2\,K$ as a function of electron concentration as shown in Fig. 2.5 for all cases of Fig. 2.3. Figure 2.6 represents the variation of the DMR with respect to alloy composition $x$ in this case.

It appears from Fig. 2.5 that the DMR of ternary materials increases with increasing carrier degeneracy. From Fig. 2.6, it appears that the DMR in ternary materials decreases with increasing alloy composition. The plots of Figs. 2.5 and 2.6 are valid for $x > 0.17$, due to the fact that for $x < 0.17$, the band gap becomes negative in n-$Hg_{1-x}Cd_xTe$ leading to a semimetallic state.

For n-$In_{1-x}Ga_xAs_yP_{1-y}$ lattice matched to InP together with the values of the energy band constants as given in Table 2.1, the DMR has been plotted as a function of electron concentration as shown in Fig. 2.7 in accordance with the three and two band models of Kane together with the isotropic parabolic energy band. It appears that the DMR monotonically increases with increasing $n_0$. Figure 2.8 shows the dependence of the DMR in n-$In_{1-x}Ga_xAs_yP_{1-y}$

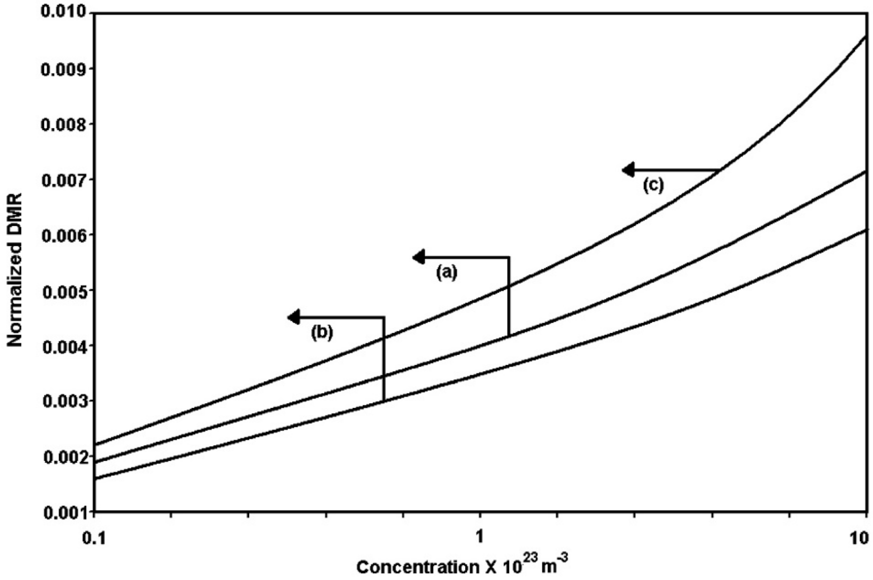

**Fig. 2.3.** The plot of the DMR in bulk specimens of n-InAs as a function of electron concentration in accordance with (**a**) the three band model of Kane, (**b**) the two band model of Kane, and (**c**) the parabolic energy bands

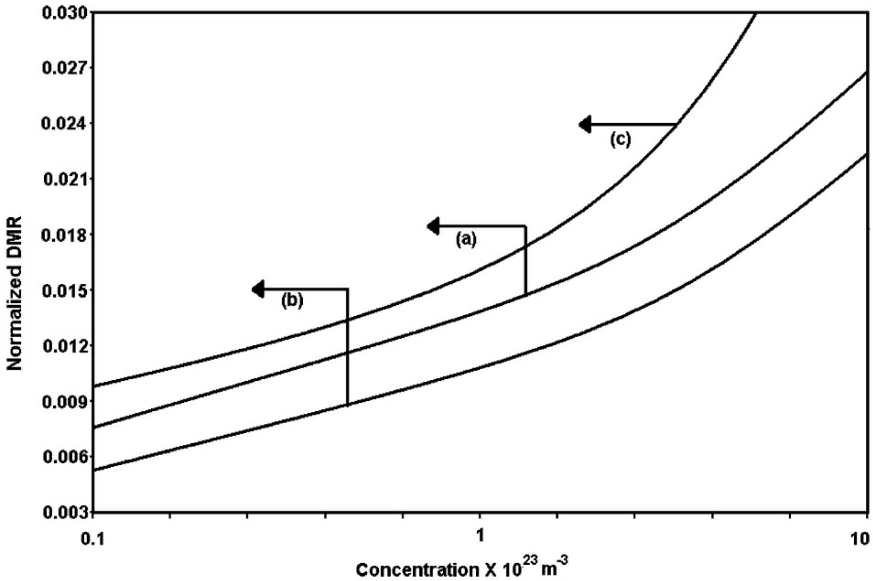

**Fig. 2.4.** The plot of the DMR in bulk specimens of n-InSb as a function of electron concentration in accordance with (**a**) the three-band model of Kane, (**b**) the two-band model of Kane, and (**c**) the parabolic energy bands

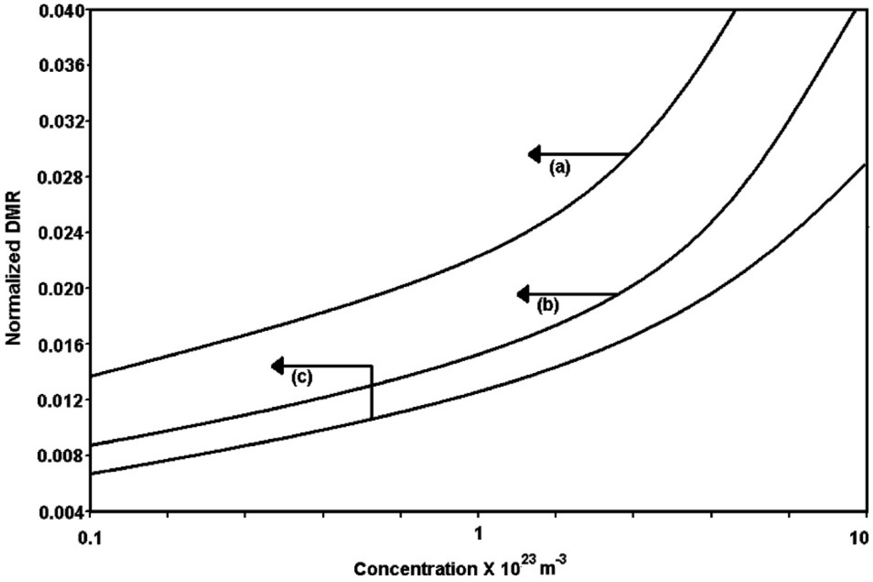

**Fig. 2.5.** The plot of the DMR in bulk specimens of n-$Hg_{1-x}Cd_xTe$ as a function of electron concentration in accordance with (**a**) the three band model of Kane; (**b**) the two band model of Kane and (**c**) the parabolic energy bands ($x = 0.3$)

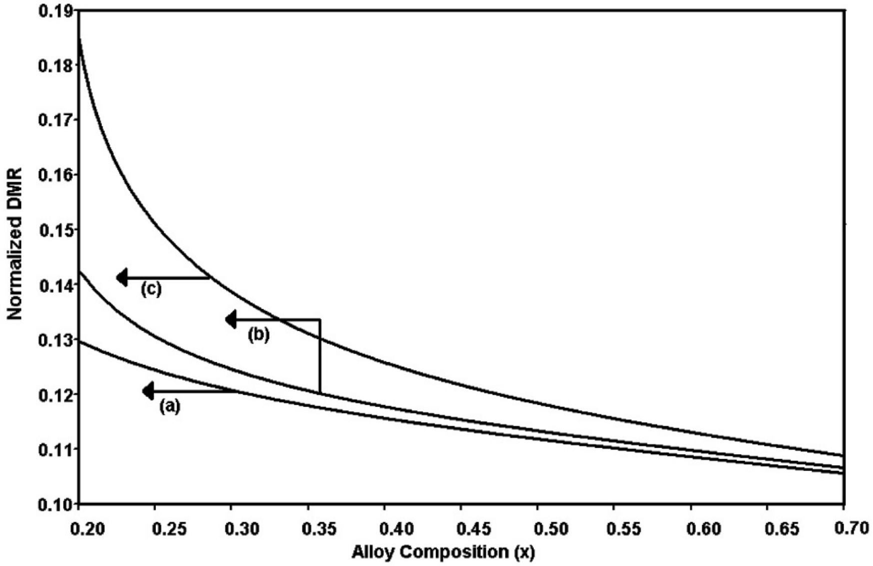

**Fig. 2.6.** The plot of the DMR in bulk specimens of n-$Hg_{1-x}Cd_xTe$ as a function of alloy composition ($x$) in accordance with (**a**) the three band model of Kane; (**b**) the two band model of Kane and (**c**) the parabolic energy bands ($n_0 = 10^{22}$ per cubic meter)

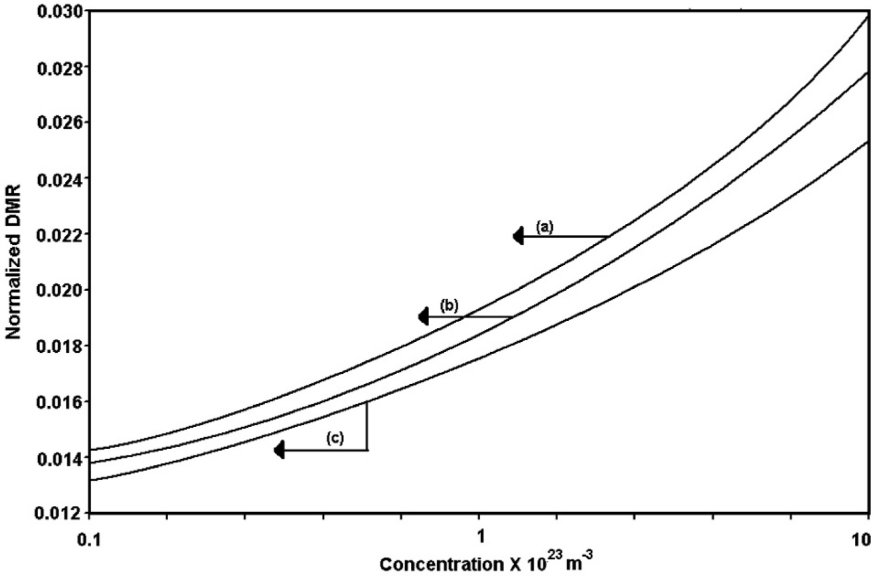

**Fig. 2.7.** The plot of the DMR in bulk specimens of n-$In_{1-x}Ga_xAs_yP_{1-y}$ lattice matched to InP as a function of electron concentration in accordance with (**a**) the three band model of Kane; (**b**) the two band model of Kane and (**c**) the parabolic energy bands ($y = 0.037$)

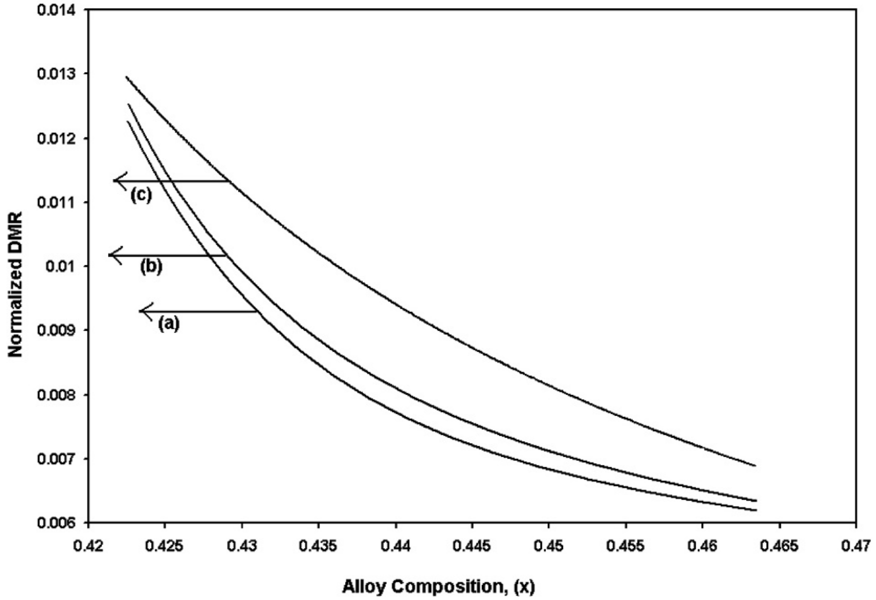

**Fig. 2.8.** The plot of the DMR in bulk specimens of n-$In_{1-x}Ga_xAs_yP_{1-y}$ lattice matched to InP as a function of alloy composition ($x$) in accordance with (**a**) the three band model of Kane; (**b**) the two band model of Kane and (**c**) the parabolic energy bands ($y = 0.037$)

lattice matched to InP on the alloy composition of $x$ for all cases of Fig. 2.6. The DMR decreases with increasing $x$ for all types of band models in this case. From Figs. 2.5 up to 2.8, one can infer the influence of energy band constants on the DMR for ternary and quaternary compounds respectively.

It may be noted that in recent years, the electron mobility in compound semiconductors has been extensively investigated, but the diffusion constant (a very important device quantity which cannot be easily determined experimentally) of such materials has been relatively less investigated. Therefore, the theoretical results presented in this chapter will be useful in determining the diffusion constants for even relatively wide gap materials whose energy band structures can be approximated by the parabolic energy bands.

We wish to point out that in formulating the basic dispersion relation we have taken into account the combined influences of the crystal field-splitting constant, the anisotropies in the effective electron masses, and the spin–orbit splitting constants, respectively, since these are the significant physical features of the tetragonal compounds.

In the absence of crystal-field splitting together with the assumptions of isotropic effective electron mass and isotropic spin–orbit splitting constant respectively, our basic equation (2.2) converts to the well-known form of the three-band model of Kane as given by (2.6). Many technologically important compounds obey the inequalities $\Delta \gg E_{\mathrm{g}}$ or $\Delta \ll E_{\mathrm{g}}$. Under these constraints, (2.6) gets simplified into (2.10) and is known as the two-band model of Kane. Finally, for $E_{\mathrm{g}} \to \infty$, as for relatively wide gap materials the above equation transforms into the well-known form $E = \hbar^2 k^2 / 2m^*$. In addition, the DMR in ternary and quaternary materials has also been investigated in accordance with the three and two band models of Kane together with the parabolic energy band for the purpose of relative assessment. Therefore, the influence of energy band constants on the DMR can also be studied from the present investigation and the basic equation (2.2) covers various materials having different energy band structures. Finally, one infers that, this simplified analysis exhibits the basic features of the DMR in bulk specimens of many technologically important compounds and for n-$\mathrm{Cd_3As_2}$, the theoretical result is in good agreement with the suggested experimental method of determining the same ratio.

## 2.2 Investigation for II–VI Semiconductors

### 2.2.1 Introduction

The II–VI compounds are being extensively used in infrared detectors [27], ultra high speed bipolar transistors [28], optic fiber communications [29], and advanced microwave devices [30]. These materials possess the appropriate direct band gap to produce light emitting diodes and lasers from blue to red wavelengths [31]. The Hopfield model describes the energy spectra of both the carriers of II–VI semiconductors where the splitting of the two-spin states by the spin orbit coupling and the crystalline field has been taken into account [32]. The DMR in II–VI compounds on the basis of the Hopfield model has been studied by formulating the expression of carrier concentration in Sect. 2.2.2. Section 2.2.3 contains the result and discussions for the numerical computation of the DMR taking p-CdS as an example.

### 2.2.2 Theoretical Background

The group theoretical analysis shows that, based on the symmetry properties of the conduction and valence band wave functions, both the energy bands of II–VI semiconductors can be written as [32]

$$E = a_0' k_s^2 + b_0' k_z^2 \pm \bar{\lambda}_0 k_s, \tag{2.27}$$

where $a_0' \equiv \frac{\hbar^2}{2m_\perp^*}$, $b_0' \equiv \frac{\hbar^2}{2m_{||}^*}$ and $\bar{\lambda}_0$ represents the splitting of the two spin-states by the spin–orbit coupling and the crystalline field.

The volume in k-space enclosed by (2.27) can be expressed as

$$V(E) = \frac{\pi}{2a_0'^2} \int\limits_{-(E/b_0')^{1/2}}^{(E/b_0')^{1/2}} \left[\bar{\lambda}_0^2 + 2a_0'E - 2a_0'b_0'k_z^2 - \bar{\lambda}_0 \left(\bar{\lambda}_0^2 - 4a_0'b_0'k_z^2 + 4a_0'E\right)^{1/2}\right] \mathrm{d}k_z, \tag{2.28}$$

From (2.28), one can write

$$V(E) = \frac{4\pi}{3a_0'\sqrt{b_0'}} \left[ E^{3/2} + \frac{3}{8}\frac{\left(\bar{\lambda}_0\right)^2 \sqrt{E}}{a_0'} - \left(\frac{3}{4}\frac{\bar{\lambda}_0}{\sqrt{a_0'}}\right)\left(E + \frac{\left(\bar{\lambda}_0\right)^2}{4a_0'}\right) \times \sin^{-1}\left[\frac{\sqrt{E}}{\sqrt{E + \frac{\left(\bar{\lambda}_0\right)^2}{4a_0'}}}\right]\right], \tag{2.29}$$

Hence, the density of states function can be written using (2.3a) and (2.29) as

$$D_0(E) = \frac{g_v}{2\pi^2 a_0' \sqrt{b_0'}} \left[\sqrt{E} - \left(\frac{\bar{\lambda}_0}{2\sqrt{a_0'}}\right) \sin^{-1}\left[\frac{\sqrt{E}}{\sqrt{E + \frac{\left(\bar{\lambda}_0\right)^2}{4a_0'}}}\right]\right]. \tag{2.30}$$

Combining (2.30) with the Fermi–Dirac occupation probability factor, the carrier concentration can be written as

$$n_0 = \frac{4\pi g_{\mathrm{v}}}{3a_0'\sqrt{b_0'}} \left[\tau_1(E_{\mathrm{F}}) + \tau_2(E_{\mathrm{F}})\right], \tag{2.31}$$

where $\tau_1(E_{\mathrm{F}}) \equiv \left[ E_{\mathrm{F}}^{3/2} + \frac{3}{8}\frac{(\bar{\lambda}_0)^2}{a_0'}\sqrt{E_{\mathrm{F}}} - \left\{ \frac{3}{4}\frac{\bar{\lambda}_0}{\sqrt{a_0'}} \left( E_{\mathrm{F}} + \frac{(\bar{\lambda}_0)^2}{4a_0'} \right) \right.\right.$

$\left.\left. \sin^{-1}\left[ \frac{\sqrt{E_{\mathrm{F}}}}{\sqrt{E_{\mathrm{F}} + \frac{(\bar{\lambda}_0)^2}{4a_0'}}} \right] \right\} \right]$, and $\tau_2(E_{\mathrm{F}}) \equiv \sum_{r=1}^{s} L(r)\,\tau_1(E_{\mathrm{F}})$.

Combining (2.31) and (1.11), the DMR in bulk specimens of II–VI semiconductors assumes the form

$$\frac{D}{\mu} = \frac{1}{|e|}\frac{[\tau_1(E_{\mathrm{F}}) + \tau_2(E_{\mathrm{F}})]}{\left[[\tau_1(E_{\mathrm{F}})]' + [\tau_2(E_{\mathrm{F}})]'\right]}, \tag{2.32}$$

Under the condition $\bar{\lambda}_0 \to 0$, (2.27) gets simplified as

$$E = a_0' k_s^2 + b_0' k_z^2, \tag{2.33}$$

Thus, under the condition $\bar{\lambda}_0 \to 0$, (2.32) reduces to the well-known form as given by (2.19).

### 2.2.3 Result and Discussions

Using (2.31) and (2.32) together with the spectrum constants as given in Table 2.1, for p-CdS, the DMR has been plotted as a function of hole concentration $p_0$ as shown by curve (a) of Fig. 2.9 in which the plot for $\bar{\lambda}_0 = 0$ (curve

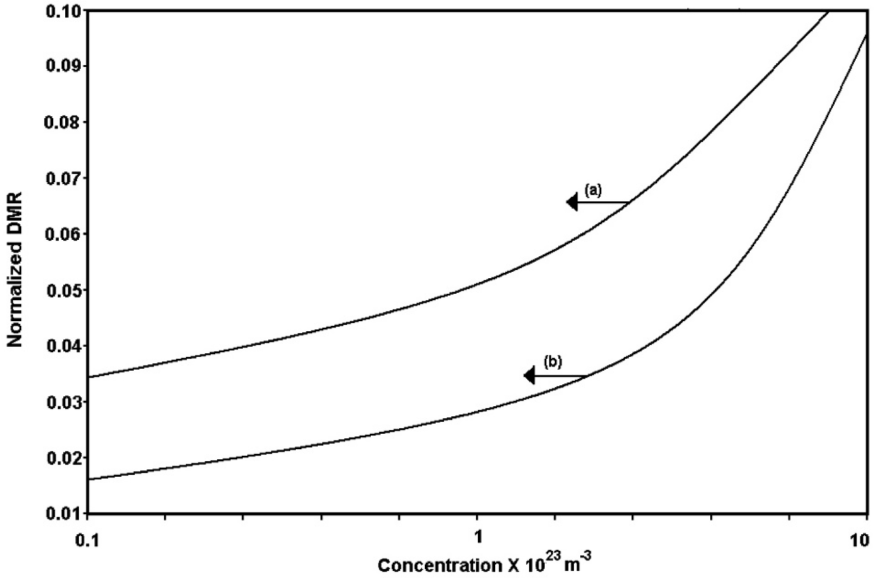

**Fig. 2.9.** The plot of the dependence of the DMR on hole concentration $p_0$ for bulk specimens of p-CdS for (**a**) $\bar{\lambda}_0 \neq 0$ and (**b**) $\bar{\lambda}_0 = 0$